analytical chemistry

pubs.acs.org/ac

Article

Solvent Precipitation SP3 (SP4) Enhances Recovery for Proteomics Sample Preparation without Magnetic Beads

Harvey E. Johnston,* Kranthikumar Yadav, Joanna M. Kirkpatrick, George S. Biggs, David Oxley, Holger B. Kramer, and Rahul S. Samant*

Cite This: *Anal. Chem.* 2022, 94, 10320−10328

Read Online

ACCESS | Metrics & More | Article Recommendations | Supporting Information

ABSTRACT: Complete, reproducible extraction of protein material is essential for comprehensive and unbiased proteome analyses. A current gold standard is single-pot, solid-phase-enhanced sample preparation (SP3), in which organic solvent and magnetic beads are used to denature and capture protein aggregates, with subsequent washes removing contaminants. However, SP3 is dependent on effective protein immobilization onto beads, risks losses during wash steps, and exhibits losses and greater costs at higher protein inputs. Here, we propose solvent precipitation SP3 (SP4) as an alternative to SP3 protein cleanup, capturing acetonitrile-induced protein aggregates by brief centrifugation rather than magnetism—with optional low-cost inert glass beads to simplify handling. SP4 recovered equivalent or greater protein yields for 1−5000 μg preparations and improved reproducibility (median protein R^2 0.99 (SP4) *vs* 0.97 (SP3)). Deep proteome profiling revealed that SP4 yielded a greater recovery of low-solubility and transmembrane proteins than SP3, benefits to aggregating protein using 80 *vs* 50% organic solvent, and equivalent recovery by SP4 and S-Trap. SP4 was verified in three other labs across eight sample types and five lysis buffers—all confirming equivalent or improved proteome characterization *vs* SP3. With near-identical recovery, this work further illustrates protein precipitation as the primary mechanism of SP3 protein cleanup and identifies that magnetic capture risks losses, especially at higher protein concentrations and among more hydrophobic proteins. SP4 offers a minimalistic approach to protein cleanup that provides cost-effective input scalability, the option to omit beads entirely, and suggests important considerations for SP3 applications—all while retaining the speed and compatibility of SP3.

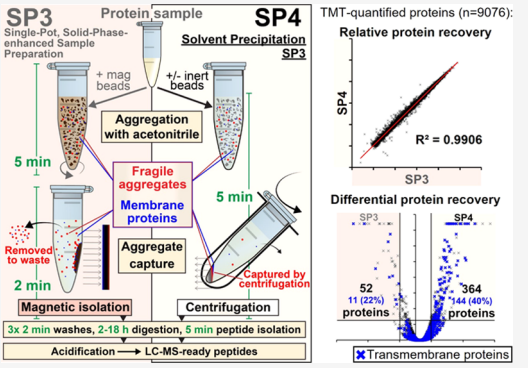

INTRODUCTION

Proteomics experiments typically aim to characterize comprehensively all proteins present in a given sample.[1] Extraction of protein material from complex biological mixtures generally requires use of buffers containing components incompatible with several stages of proteomics analysis (*e.g.*, detergents, salts).[2] Although several cleanup methods exist,[3−6] contaminant removal represents a major source of sample losses and experimental variability.[7]

An increasingly popular sample preparation method is SP3 (single-pot, solid-phase-enhanced sample preparation), employing a single reaction vessel, carboxylate-modified magnetic beads (CMMBs), and organic solvent-induced protein aggregation to wash away contaminants.[5,8−10] SP3 is a fast, effective, high-throughput, and relatively streamlined protocol—compatible with automation and a range of protein inputs, with diverse proteomics applications.[5,11−16] Improvements on the initially proposed protein cleanup method include neutral pH, solvent adjustments, and a more rapid workflow taking around 90 min from cells to peptides.[5,10,11]

However, SP3 has the potential for losses and variability, *e.g.*, if protein aggregates do not completely adhere to magnetic beads, if aggregates are disrupted during wash steps, or if technical steps are not followed carefully.[9] Larger protein inputs (*e.g.*, for enrichment of post-translational modifications (PTMs)) are also disadvantaged by counter-intuitive losses and bead costs.[5,11] Furthermore, CMMBs present a physical contamination risk and the potential to bind protease inhibitors.[14]

Although the mechanism of SP3 was originally proposed to involve hydrophilic interaction chromatography (HILIC)-like solid-phase interaction between CMMBs and proteins, Batth et al. recently demonstrated that protein recovery for SP3 is not dependent on bead surface chemistry.[13] Their work suggests that HILIC-like interactions are not the primary form of solid-phase bead−protein interactions. Instead, the authors described the SP3 mechanism as protein aggregation capture

Received: September 27, 2021
Accepted: June 26, 2022
Published: July 18, 2022

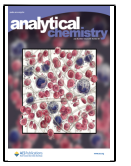

Downloaded via 67.180.9.111 on January 7, 2023 at 23:04:34 (UTC).
See https://pubs.acs.org/sharingguidelines for options on how to legitimately share published articles.

ACS Publications

© 2022 The Authors. Published by American Chemical Society

(PAC), driven by organic solvent-induced denaturation. PAC, and therefore SP3, bear a striking mechanistic similarity to protein precipitation—a well-established purification approach that typically employs organic solvents to induce protein denaturation and precipitation into insoluble aggregates. However, protein precipitation has historically been associated with extended incubation steps, incomplete protein capture, and chemical modification of proteins and/or peptides.[17−21] Nevertheless, several recent methods have demonstrated that combining protein precipitation with filter-based trapping provides a rapid means of protein capture and cleanup.[22−24] The importance of ionic strength (>10 mM NaCl) was demonstrated to be essential for protein precipitation, allowing the reaction to complete in as little as 2 min.[25]

Building upon the SP3 developments of Batth et al.,[13] here we omit magnetic beads entirely and instead employ acetonitrile (ACN)-induced protein precipitation and centrifugation for protein capture and isolation—either bead-free (BF), or with low-cost, inert glass beads (GB). We name this method SP4 or *S*olvent *P*recipitation SP3. Both SP4 variants matched or outperformed SP3 across a variety of applications and settings, with SP4-GB offering technical advantages and some higher recovery than SP4-BF. SP4 also yielded equivalent results to S-Trap. We provide further evidence that protein precipitation is the primary mechanism of SP3 protein enrichment. We therefore propose that CMMBs, while advantageous in specific settings (*e.g.*, peptide fractionation and automation[14−16]), can be replaced with inert glass beads—or omitted altogether—without adversely affecting proteome recovery, provided protein input and concentration are sufficiently high (>1 μg and >0.25 μg/μL, respectively). Furthermore, magnetic capture in SP3 increased the risk of protein aggregate losses—especially of low-solubility (*e.g.*, membrane) proteins and at higher protein concentrations. SP4 offers a minimalistic, low-cost protein cleanup approach (especially for high-input preparations, *e.g.*, prior to PTM analyses), is easy to use for non-proteomics scientists, requires no specialized equipment or reagents, offers the option to omit beads entirely, and improves recovery of hydrophobic proteins—while retaining the speed and broad compatibility of SP3.

METHODS

SP3/SP4 Preparations. Full methods and materials are provided in the Supporting Information, alongside a detailed step-by-step protocol. HEK293 cells were lysed using trituration in "SP3 lysis buffer" (50 mM HEPES pH 8.0, 1% SDS, 1% Triton X-100, 1% NP-40, 1% Tween 20, 1% sodium deoxycholate, 50 mM NaCl, 5 mM EDTA, 1% (v/v) glycerol) supplemented with 10 mM DTT, 1× cOmplete protease inhibitor, and 40 mM 2-chloroacetamide, followed by heating at 95 °C for 5 min and sonication on ice for 12 × 5 s bursts. Lysates were adjusted to 5 μg/μL. Silica beads/glass spheres (9−13 μm mean particle diameter; Sigma catalogue no. 440345) were suspended at an initial concentration of 100 mg/mL in Milli-Q water, washed sequentially with ACN, 100 mM ammonium bicarbonate (ABC), and 2× with water, pelleted at 16,000*g* for 1 min, and the supernatant was discarded (also removing any unpelleted beads). Glass beads were adjusted to a final concentration of 50 mg/mL in water or 12.5 mg/mL in ACN. A 10:1 bead/protein ratio for SP3 and SP4-GB, or an equivalent volume of water for SP4-BF experiments, was added to lysates and gently mixed at 400 rpm. Then, 4 volumes of 100% ACN was added, and tubes were mixed for 5 s at 400 rpm. Alternatively, glass beads were added to lysate presuspended in ACN. SP3 samples were incubated at 25 °C for 5 min at 800 rpm on a Thermomixer Comfort and placed on a magnetic rack for 2 min. SP4 samples were centrifuged for 5 min at 16,000*g*. Supernatants were aspirated and carefully washed 3× with 80% ethanol. Each wash used either a 2-min magnetic separation (SP3) or 2-min centrifugation at 16,000*g* (SP4, cSP3). Protein aggregates were digested with 1:100 trypsin:protein ratio in 100 mM ABC for 18 h at 37 °C at 1000 rpm on a Thermomixer Comfort. For TMT labeling, 100 μg of protein was processed, and 100 mM triethylammonium bicarbonate (TEAB) with 1:100 trypsin and Lys-C were added. Peptide solutions were isolated by removal of magnetic beads (MagRack and 16,000*g*, SP3) or beads and insoluble debris (16,000*g*, SP4) for 2 min. Peptide yields for optimization were assessed using the Pierce Quantitative Fluorometric Peptide Assay (Thermo Scientific) according to the manufacturer's instructions. After digestion, peptides were acidified with 2% ACN and 0.1% trifluoroacetic acid and were sufficiently clean for LC-MS injection.

S-Trap, Spin Filter, and SP4 Protein Cleanup. HEK293 lysate was prepared with 5% SDS and 50 mM TEAB as recommended by the S-Trap mini protocol. Briefly, 100 μg of the same lysate was processed for all samples (n = 4, label-free; n = 2, TMT). For S-Trap, the manufacturer's recommended protocol was followed for mini columns. For spin filtration, a nylon 0.22 μm spin filter was used to capture the precipitate. For SP4-GB, the protein was precipitated with an ACN−bead suspension, and the described SP4 protocol was followed. Digests were performed with 5 μg of trypsin and 2 μg of Lys-C in 125 μL of 50 mM TEAB for 2 h. Peptide solutions were lyophilized and reconstituted in 100 μL of 100 mM TEAB.

TMT Labeling and Peptide Fractionation. Briefly, 100 μg of peptides were labeled with 0.2 mg of TMT labeling reagent according to the manufacturer's instructions. Labeled peptides were vacuum-concentrated, then reconstituted, pooled, and resolved using high-pH RP C18 chromatography over a 105-min gradient.

LC-MS Acquisition and Analysis. Label-free analyses of peptides were acquired over 120 min by a Q-Exactive Plus Orbitrap MS (Thermo Scientific) from 100 ng of peptides (as a proportion of protein input). TMT-labeled peptide fractions were analyzed over 60 or 120 min by an Orbitrap Eclipse MS (Thermo Scientific) using SPS MS^3 mode. Raw files were processed and analyzed with Proteome Discoverer 2.5, searching against UniProt Swiss-Prot (version 2021_01, canonical). Additional analysis was performed in Microsoft Excel. The MS proteomics data have been deposited to the ProteomeXchange Consortium (http://proteomecentral.proteomexchange.org) via the PRIDE partner repository[26] with the data set identifier PXD032095 and, for validation work, PXD028736 and PXD028768. Proteomics data are detailed in Tables S1−S20. Annotation enrichment was performed with DAVID and PANTHER. Additional analyses were performed with CamSol,[27] the PROMPT tool,[28] and Proteome-pI.[29]

RESULTS

Single-Pot Solvent Precipitation with Acetonitrile Provides Effective Protein Capture and Cleanup. Building on previous mechanistic observations of SP3, we wanted to explore further the hypothesis that protein capture

https://doi.org/10.1021/acs.analchem.1c04200
Anal. Chem. 2022, 94, 10320−10328

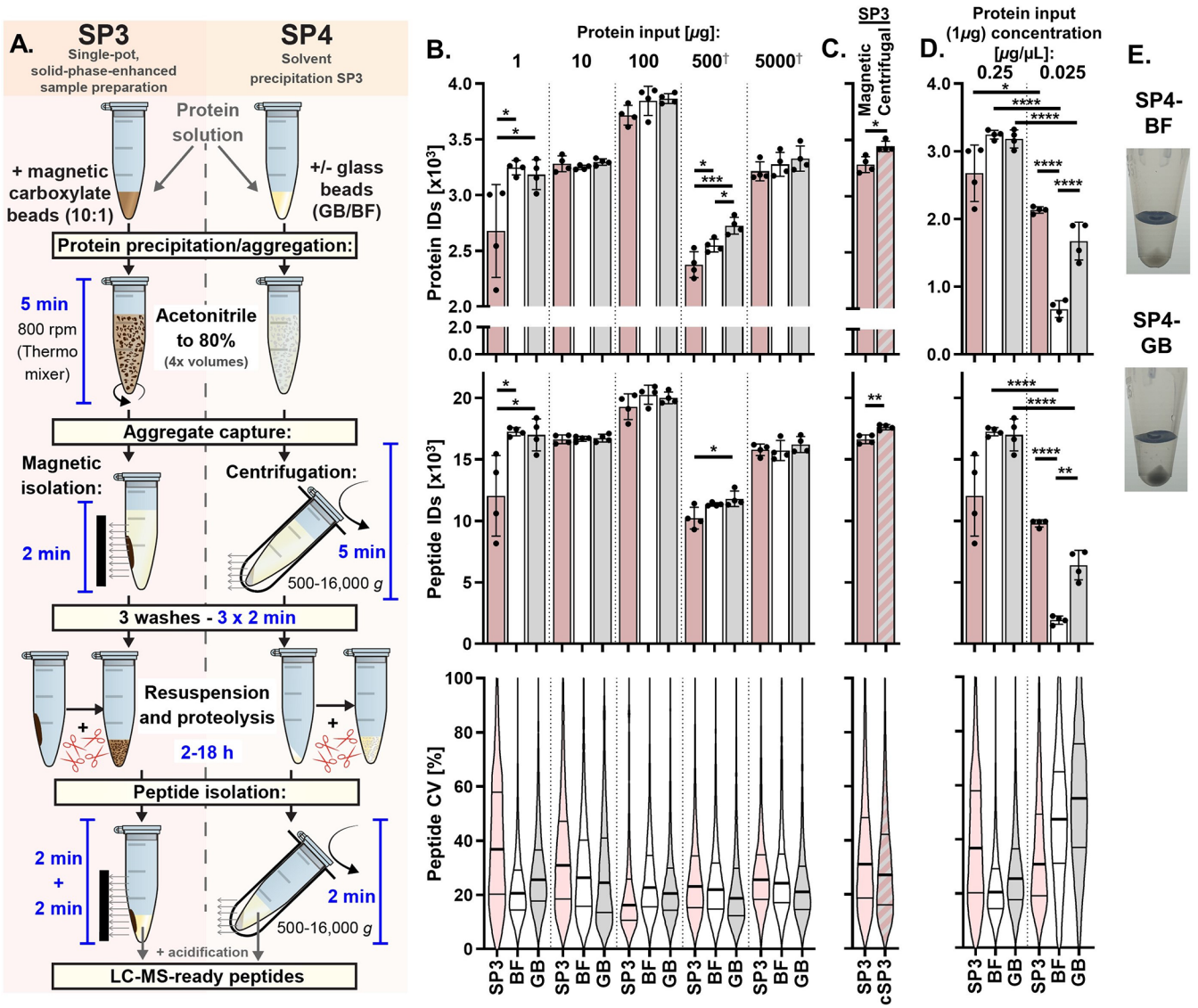

Figure 1. Comparison of SP3 with SP4. (A) Summary of the SP3 and SP4 workflows. For both approaches, protein in solution is aggregated with acetonitrile in the presence of carboxylate-modified magnetic beads (SP3), glass beads (SP4-GB), or bead-free (SP4-BF), captured by magnetism (SP3) or centrifugation (SP4), and contaminants removed with 3 washes prior to protein digestion—yielding peptides sufficiently clean for LC-MS injection. (B) Protein and peptide identifications and peptide coefficient of variance (CV) (as violin plots; thick line—median, thin lines—quartiles) for 1—5000 μg preparations of HEK293 cell lysate by SP3, SP4-BF, and SP4-GB (n = 4). Protein concentrations were 0.25 μg/μL for 1 and 10 μg (in 4 and 40 μL) and 2.5 μg/μL for 100, 500, and 5000 μg (in 40, 200 and 2000 μL). A 10:1 bead:protein ratio was used in all SP3 and SP4-GB experiments. †500 and 5000 μg preparations were digested with TrypZean instead of MS-grade trypsin. (C) Aliquots of 10 μg of protein processed with carboxylate-modified magnetic beads and captured by either standard magnetic capture (SP3) or centrifugal (16,000g) SP3 (cSP3) (D) Aliquots of 1 μg of protein preparations processed at 0.025 and 0.25 μg/μL. (E) Aliquots of 50 μg of protein precipitated in the presence of 500 μg (10:1) of glass beads, offering increased pellet visibility and definition *vs* bead-free precipitation. Bar charts present median and standard deviation, with significance assessed by ANOVA (B, D) and t-test (C). Protein coefficients of variance distributions represented by violin plots (thick line—median, thin lines—quartiles). *p < 0.05, **p < 0.01, ***p < 0.001, ****p < 0.0001, and ns—not significant.

observed in SP3 is primarily a product of solvent-induced denaturation, aggregation, and subsequent precipitation, rather than being dependent on bead surface chemistry.[13] We noticed that 80% ACN, similar to the conditions used to aggregate proteins during SP3, is also employed in the effective exclusion of proteins from peptidomics and metabolomics analyses through precipitation—termed a protein 'crash.'[30−33] As magnetic capture risks losses from incomplete, fragile, or disrupted aggregate adhesion, and 80% ACN effectively precipitates proteins, we hypothesized that centrifugation-based capture could be combined with aspects of the SP3 protocol to provide a more effective means of sample cleanup for proteomics (Figures 1A and S1). The protocol was also adapted to incorporate many of the recent optimizations to SP3, including neutral pH, higher ACN concentration for aggregation, and no reconstitution of the protein—bead aggregates.[5,10,11]

We named our optimized protocol SP4, or Solvent Precipitation SP3. Two variants were devised: one without any beads (bead-free, SP4-BF), thus relying on precipitation alone, and a second with inert, low-cost silica particles (hereafter termed glass beads, SP4-GB), allowing us to explore the role of surface area independently of bead chemistry. Initially, a broad range of SP4 parameters were evaluated by

https://doi.org/10.1021/acs.analchem.1c04200
Anal. Chem. 2022, 94, 10320−10328

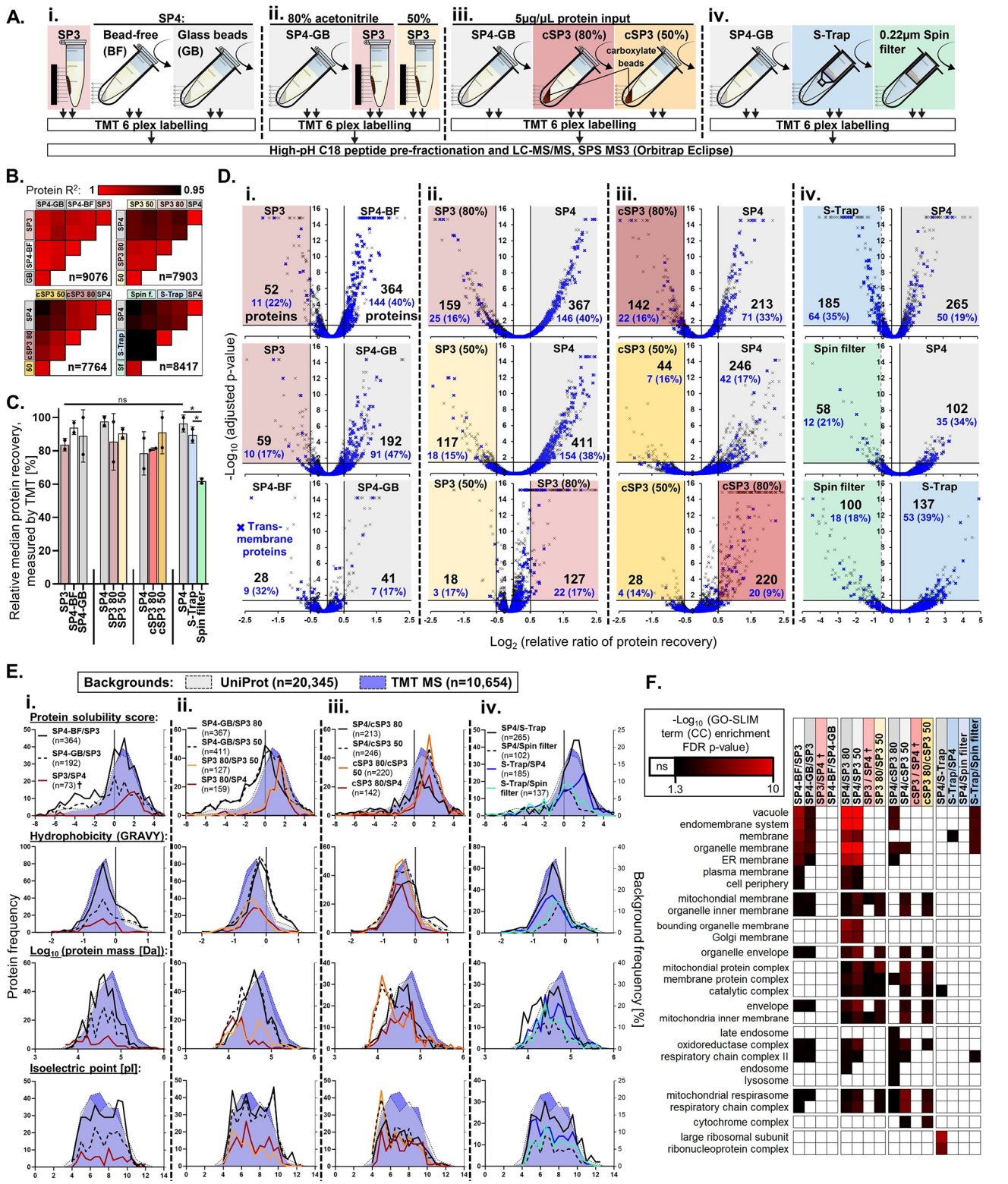

Figure 2. Deep proteome profiling comparing SP3, SP4, and other protein precipitation methods by isobaric labeling. (A) Experimental workflows applied to compare variants of SP3, SP4, and other protein precipitation capture methods to a high depth of proteome coverage. (B) Correlation between protein abundances for sample preparation method replicates. (C) Relative protein recovery percentages determined within each 6-plex across method replicates ($n = 2$) derived from TMT quantitation values. *$p < 0.05$. (D) Volcano plots indicating more effective protein recovery (adjusted $p < 0.05$ and $\log_2$ (fold change) > 0.5) by each of the preparation approaches. Blue crosses and numbers represent transmembrane proteins and their proportion of the differentially recovered proteins. (E) Frequency distributions of physical properties among proteins with significantly greater recovery (defined in (D)). Both the human UniProt Swiss-Prot (gray) and the MS-derived TMT (blue) proteomes are displayed as percentage frequency backgrounds. See also Figure S7. (F) Cellular component GO-SLIM term enrichment analysis of proteins more effectively isolated by each method (defined in (D)). †Protein lists were combined for these analyses, *e.g.*, SP3/SP4 = SP3/SP4-BF and SP3/SP4-GB.

https://doi.org/10.1021/acs.analchem.1c04200
Anal. Chem. 2022, 94, 10320−10328

peptide yield, including 40−95% ACN, 0:1−160:1 glass bead:protein ratios, and 0.5−20 min centrifugation times (Figure S1). These experiments demonstrated that parameters equivalent to SP3, i.e., 80% ACN, a 10:1 glass bead:protein ratio, and 5- and 2-min protein capture steps were also the most effective for SP4—and provided peptides ready for LC-MS without any further cleanup required. Therefore, rapid protein aggregate capture by centrifugation-based SP4 provides a potential option for the preparation of samples for proteomics analysis.

Centrifugation Outperforms Magnetic Capture of Solvent-Induced Protein Aggregates. To evaluate how the capture of protein aggregates by centrifugation compared with magnet- and CMMB-based SP3, 1−5000 μg of HEK293 cell lysate was processed by SP3, SP4-BF, and SP4-GB (Figures 1B and S2 and Tables S2−S6). Both variants of SP4 consistently either matched or exceeded the number of protein and peptide identifications of SP3 across the range of evaluated inputs. A mean of 3036, 3275, 3810, 2549, and 3272 proteins were identified for the 1, 10, 100, 500, and 5000 μg input experiments, respectively. On average, more proteins were observed for the 1, 100, 500, and 5000 μg inputs for SP4-BF (+569 ($p < 0.05$), +129, +172, ($p < 0.05$), and +63 proteins, respectively) and SP4-GB (+506 ($p < 0.05$), +149, +350 ($p < 0.01$), and +114) *vs* SP3, with the 10 μg experiment showing roughly equivalent protein numbers (SP3: 3281; SP4-BF: 3248; and SP4-GB: 3297, Figure 1B and Table S1). Peptide identifications (Figure 1B) and other measures of proteome quality (Figure S2) also consistently indicated greater or equivalent protein recovery by SP4. Quantitative reproducibility was also assessed, with coefficients of variation (CV, Figure 1B) indicating at least equivalent or greater reproducibility for SP4 in the 1, 10, 500, and 5000 μg comparisons. Median protein R^2 values were 0.970, 0.980, and 0.993 for SP3, SP4-BF, and SP4-GB, respectively (Figure S3). For both SP4 methods, more proteins demonstrated significantly greater recovery (fold change (FC) > 2 and adjusted $p < 0.05$) *vs* SP3, with SP4-GB offering additional recovery for all inputs (Figure S4). A slight trend of greater recovery of transmembrane proteins was apparent in these data (Figure S4). The inclusion of glass beads also offered some marginal increases to mean protein identifications *vs* SP4-BF for the 10, 100, 500, and 5000 μg (49, 20, 179 ($p < 0.01$), and 52, respectively), alongside lower CVs in these samples. Missed cleavages were reduced in all but the lowest input (1 μg) for SP4-GB relative to SP3, and for all but the lowest and highest (1 and 5000 μg) inputs relative to SP4-BF (Figure S2).

Next, to evaluate the hypothesis that some proteins were not fully aggregating or captured by CMMBs in SP3, the SP3 protocol was performed with centrifugation in place of magnetic capture ("cSP3") (Figures 1C and S5). cSP3 outperformed magnetic capture of protein−bead aggregates, with significantly increased protein (+215, $p < 0.05$) and peptide (+1492, $p < 0.01$) identifications.

The previously noted[13] effects of protein concentration on SP3 and SP4 were also investigated. Recovery from 0.025 *vs* 0.25 μg/μL protein sample concentrations (Figure 1D) indicated that, although the 10-fold dilution caused significant losses in all three workflows, the losses were far greater for SP4-BF (3246 *vs* 669, $p < 0.0001$) and SP4-GB (3184 *vs* 1674, $p < 0.0001$) than for SP3 (2678 *vs* 2135 proteins, $p < 0.05$). Each 2-fold protein dilution indicated an approximate 15 and 20% loss of recovered peptides for SP3 and SP4, respectively (Figure S1C). Our results highlight an important limitation of SP4, with SP3 providing superior recovery for low-concentration samples.

While the advantages of SP4-GB over SP4-BF were generally marginal, the addition of glass beads offered several technical advantages, most notably increasing the visibility, definition, density, and ease of resuspension of the protein pellet (Figure 1E).

Finally, several additional aspects of SP4 were investigated, identifying similar yields using acetone instead of ACN for precipitation (Figure S5B), superior peptide yield at lower centrifugation speeds (Figure S5D), and broad compatibility with alternative, detergent-free lysis approaches such as trifluoroacetic acid in the "Sample Preparation by Easy Extraction and Digestion" (SPEED) protocol[23] (Figure S5E) and urea (Figure S5F).

Together, these findings suggest that centrifugation-based protein aggregate capture by SP4 offers robust advantages over dependence on CMMB−aggregate interactions of SP3 (except in circumstances where protein concentration is very low) and confirm its compatibility across a broad range of cell lysis and aggregate-capture parameters.

Deep Proteome Profiling Identifies Superior Recovery of Membrane and Low-Solubility Proteins by SP4. To understand better the nature and mechanisms of proteins not captured by SP3, we next evaluated the proteins recovered by SP3 and SP4 to a higher depth by isobaric labeling and off-line peptide fractionation (Figure 2A-i). Briefly, 100 μg of peptides were prepared in duplicate by SP3, SP4-BF, and SP4-GB, labeled with TMT 6-plex and characterized by two-dimensional (2D) LC-MS/MS using synchronous precursor selection (SPS) and MS^3 quantification. With this approach, we were able to evaluate quantitatively the recovery of peptides matching 9076 proteins.

Protein recovery had high inter- and intra-method correlations (R^2 > 0.98 and 0.99, respectively) (Figures 2B and S6), with SP4 indicating a marginally higher median protein yield than SP3, as measured by TMT (Figure 2C). Compared with SP3, 364 and 192 proteins had significantly higher recovery ($\log_2$(FC) > 0.5, $p < 0.05$) for SP4-BF and SP4-GB, respectively (Figure 2D-i). Only 73 proteins had a greater recovery by SP3 *vs* SP4 (BF or GB). Very little differential recovery was observed between the BF and GB SP4 variants (28 and 41 proteins, respectively). The physicochemical properties of differentially recovered proteins highlighted a significant enrichment of hydrophobic and lower-solubility proteins (p < 0.0001) by both SP4 variants *vs* SP3 (Figures 2E-i and S7). Annotation enrichment additionally identified several terms descriptive of membrane proteins for SP4 (Figures 2F and S6), such as "membrane" (n = 221/364, $p = 2.4 \times 10^{-5}$) and "intrinsic component of membrane" (n = 153/364, $p = 7.9 \times 10^{-14}$) (Figure S6). For SP4-BF and SP4-GB, 40 and 47% (144/364 and 91/192) were annotated as transmembrane proteins, respectively (Figure 2D-i, blue crosses)—almost three times the background rate observed by LC-MS (16%).

Given previous suggestions that lower organic conditions be used for SP3-based aggregation,[9] we compared 50 *vs* 80% ACN for SP3 and SP4-GB (Figure 2A-ii). This experiment reflected the findings of the first 6-plex, with SP4 offering greater differential recovery of proteins (411 and 367 proteins ($\log_2$(FC) > 0.5, $p < 0.05$), Figure 2D-ii), transmembrane proteins (146 and 154, Figure 2D-ii), hydrophobic proteins (p

https://doi.org/10.1021/acs.analchem.1c04200
Anal. Chem. 2022, 94, 10320−10328

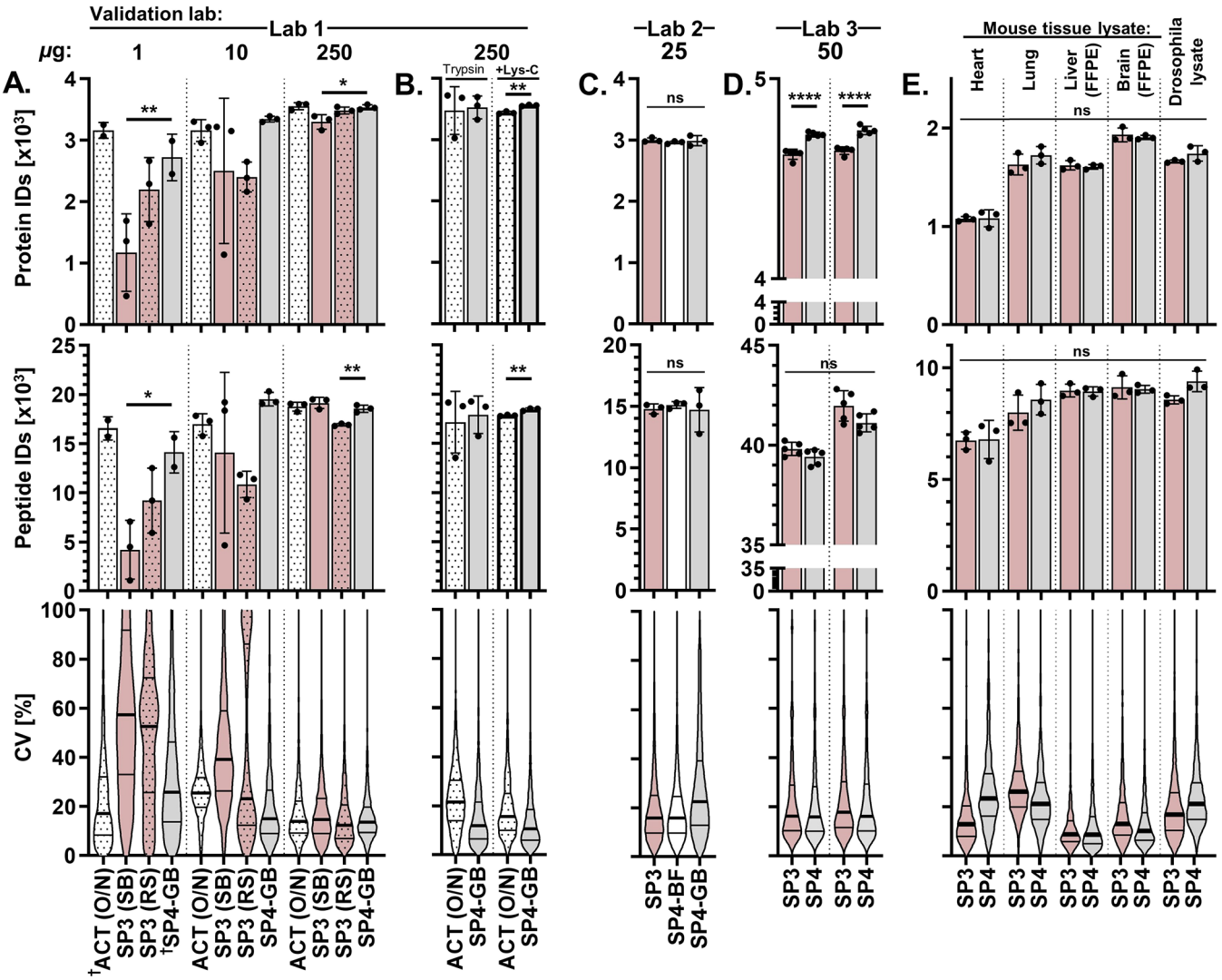

Figure 3. Independent method validations and complex applications of SP4 cleanup for proteomics. The SP4 protocol was provided to three collaborators and applied to several sample types to compare SP4 with SP3. (A) Lab 1 performed SP3 with either SpeedBeads carboxylate or ReSyn HILIC magnetic beads compared with overnight acetone (ACT(O/N)) precipitation and SP4-GB for 1, 10, and 250 μg preparations of Jurkat human immortalized T cell lysate (n = 3). †n = 2; see Supporting Methods. (B) Acetone precipitation and SP4 were compared for 250 μg HEK293 lysate digested with trypsin +/− Lys-C. (C) Lab 2 processed 25 μg of HEK293 lysate for SP3, SP4-BF, and SP4-GB protocols. (D) Lab 3 processed two independent n = 5 comparisons of SP3 and SP4-GB using 50 μg of E14 murine embryonic stem cell lysate. (E) SP3 and SP4 preparations of more complex lysates/homogenates derived from whole organs, organisms, and formalin-fixed paraffin-embedded (FFPE) tissue. Bar charts present median and standard deviation, with significance assessed by ANOVA (A, C) and t-test (B, D, E). Protein coefficients of variance distributions represented by violin plot (thick line−median, thin lines−quartiles). *p < 0.05, **p < 0.01, ***p < 0.001, ****p < 0.0001, and ns−not significant.

< 0.0001, Figures 2E-ii and S7), and "membrane"-annotated proteins (p < 0.0001, Figure 2F-ii) *vs* SP3 using 80 and 50% ACN, respectively. Importantly, these observations for SP4 held true *vs* SP3 at either ACN concentration and were more pronounced when compared to 50% ACN. Losses of low-molecular-weight and soluble proteins were apparent for the use of 50 *vs* 80% ACN for SP3 (p < 0.0001, Figures 2E-ii and S7), among those 127 proteins exhibiting significantly lower recovery ($\log_2$(FC) > 0.5, p < 0.05, Figure 2D-ii).

SP3 (80% ACN) demonstrated a greater recovery of lower-than-median molecular weight proteins (52 and 98, p < 0.0001) and higher-than-median solubility proteins (56 and 114, p < 0.0001) *vs* SP4 in both TMT experiments (Figure 2E-i,E-ii, respectively). However, generally, higher numbers of lower-than-median solubility proteins (208, 116, and 255, p < 0.0001) and transmembrane proteins (144, 91, and 146) had greater recovery for SP4-BF, SP4-GB (TMT-i) and SP4-GB (TMT-ii), respectively, *vs* SP3 (Figure 2D,E).

To determine whether lower membrane protein yields in SP3 resulted from fragile aggregates being lost during magnetic capture, SP4-GB was compared with centrifugal SP3 (cSP3) in a third TMT 6-plex, again using both 80 and 50% ACN for SP3. This experiment also offered insight into the impact of CMMB presence during precipitation, independent of the capture method (magnetic or centrifugal). As CMMBs appeared to offer an increased concentration of surrogate nucleation points (Figures 1D and S1C), we attempted to minimize this effect using a high concentration of protein (5 μg/μL)—theoretically providing ample nucleation points across all three conditions.

cSP3 with 80% ACN matched SP4 in most measures, with consistent median recovery (Figure 2C) and reproducibility

https://doi.org/10.1021/acs.analchem.1c04200
Anal. Chem. 2022, 94, 10320−10328

(R^2 = 0.9966 (cSP3-80%) *vs* 0.9941 (SP4-GB)) (Figure 2B) and balanced differential recovery (142 (cSP3-80%) *vs* 213 (SP4-GB) proteins) between the methods (Figure 2D-iii). Less than half the number of membrane proteins exhibited losses for cSP3-80% (n = 71) (Figure 2D-iii) *vs* magnetic SP3 (n = 146) (Figure 2D-ii), although some enrichment for SP4-GB remained *vs* cSP3.

The use of 50% ACN with cSP3 also presented greater losses of specific proteins *vs* 80% ACN (n = 220, $\log_2$(FC) > 0.5, p < 0.05, Figure 2D-iii), especially those with lower isoelectric points and molecular weights (p < 0.0001, Figures 2E-iii and S7). For all comparisons to SP3, cSP3, and SP4 (all using 80% ACN), the use of 50% ACN resulted in the less efficient capture of low-molecular-weight and high-solubility proteins (Figure 2D-ii,D-iii). It is worth noting that cSP3-50% indicated a marginally higher median total protein yield (based on summed intensities of all TMT quantitations) relative to SP3 and SP4 using 80% ACN (Figure 2C), but this did not translate to a greater recovery of many specific proteins (n = 28, $\log_2$(FC) > 0.5, p < 0.05, Figure 2D-iii).

Taken together, our analysis indicates that centrifugation offers a more effective means of aggregate capture than magnetism, especially among membrane and other low-solubility proteins. When protein input and concentration are sufficient and centrifugation is an option, CMMBs can be omitted during aggregate capture in many applications.

SP4 Matches the Performance of S-Trap. To understand the performance of SP4 versus other protein cleanup methods, a further fractionated 6-plex (Figure 2A-iv) was employed—alongside a label-free analysis (Figure S9, n = 4)—to compare the deep proteome (n = 8417) recoveries of protein precipitate captured by SP4 *vs* two filtration-based aggregate-capture approaches: S-Trap, and 0.22 μm spin filters.[22,23] SP4 matched S-Trap in most measures, with 265 *vs* 185 (50 *vs* 64 transmembrane) proteins, respectively, exhibiting significantly higher recovery ($\log_2$(FC) > 0.5, p < 0.05, Figure 2D-iv), consistent reproducibility (R^2 = 0.9970 *vs* 0.9964, Figure 2B), and a marginally higher median recovery for SP4 (Figure 2C). For S-Trap *vs* SP4, protein property distributions were skewed toward trends of higher recovery for high-solubility proteins, lower recovery of low-molecular-weight proteins (Figure 2E-iv), and significantly lower recovery of "ribonucleoproteins" (n = 21/265, $p = 2.0 \times 10^{-7}$, Figures 2F and S8). For label-free, SP4 identified significantly more peptides than S-Trap (p < 0.05) but offered lower CVs% (Figure S9). Spin filters exhibited significantly lower recovery (<70% of SP4 or S-Trap, p < 0.05) and reproducibility across both the TMT and label-free experiments (Figures 2B,C and S9). Overall, SP4 and S-Trap appear to provide broadly similar results, whereas the use of spin filters risks losses.

SP4 Matches or Outperforms SP3 Independent of User and Sample Type. To confirm that SP4 was not dependent on any single user, setting, or sample complexity, the protocol was shared with three collaborators and applied to lysates from several sources (Figure 3). Lab 1 found that SP4-GB consistently performed effectively across a range of protein inputs, matching or outperforming SP3 with two magnetic particles (ReSyn (RS) HILIC or SpeedBeads (SB) carboxylate beads) and overnight acetone precipitation (Figure 3A), especially when additionally digesting with Lys-C (Figure 3B). Lab 2 prepared 25 μg of HEK293 lysate in triplicate and found SP3, SP4-BF, and SP4-GB roughly equivalent (Figure 3C). Lab 3 compared SP3 and SP4-GB with two independent (n = 5) comparisons of 50 μg of mouse E14 embryonic stem cell lysate. For both experiments, approximately 100 more proteins were identified by SP4-GB (p < 0.001), even though the number of peptides did not significantly differ between comparisons (p > 0.05, Figure 3D). We also performed SP4 *vs* SP3 on more complex samples, including lysates derived from whole mouse organs, formalin-fixed paraffin-embedded (FFPE) tissue preparations, and whole *Drosophila melanogaster*, to confirm the broad utility of SP4 (Figure 3E,F). Importantly, no significant differences were observed between the two methods (p > 0.05). These experiments further demonstrate that the SP4 protocol consistently either matches or outperforms SP3 independent of user, setting, or application.

DISCUSSION

SP3 is one of the most effective means of proteomics sample capture and cleanup currently available. However, its reliance on stable aggregation of proteins onto magnetic beads remains a potential source of variability and loss. By evaluating centrifugation of protein aggregates with SP4—with or without glass beads—we show that losses exhibited by SP3 can be reduced and that CMMBs are not required for effective protein aggregate capture for many applications. SP4 robustly offered greater or equivalent protein and peptide identifications *vs* SP3 across a broad range of conditions, including 1−5000 μg of protein input, eight sample types, five lysis buffers, and four lab settings that use a diverse range of downstream proteomics methods.

Generally, SP3 and SP4 provided highly comparable proteomics options, with both offering a rapid single-pot protein capture and cleanup protocol, broad compatibility, and the option to elute LC-MS-ready peptides. Each method, however, offered different advantages for protein cleanup. While SP3 performed better at very low protein concentrations (*e.g.*, 0.025 μg/μL, Figure 1F) and for a subset of low-molecular-weight proteins (Figure 2E-ii.), SP4 matched or outperformed SP3 at the higher concentrations used in this study (0.25−5 μg/μL)—especially among proteins with low solubility, high hydrophobicity, and transmembrane domains (Figure 2D−F). Additionally, SP4 requires no specialized reagents or equipment, allows rapid preparations with or without beads, and offers low-cost, high-input scalability to preparations beyond the recommended 300 μg limit for SP3.[9] SP4 therefore provides a more robust and effective means of protein cleanup for global proteomics studies compared to SP3, especially when a high protein concentration is available (>0.25 μg/μL) and marginal losses to some smaller, soluble proteins are tolerable.

In most instances, glass beads provided some (albeit limited) improvement to proteomics outputs *vs* SP4-BF; however, their most notable advantages were technical. Glass beads outcompeted tube walls as a precipitation surface, promoted a more defined, visible, and stable precipitation pellet (Figure 1E), facilitated pellet resuspension, and offered fewer missed cleavages (Figure S2). They also present greater chemical and freezing compatibility and substantially lower cost (~1/1000th) than CMMBs. When tested, SP4-GB was also found to be compatible with 2 h digestions (Figures 2A-iv and 3D). Presuspending the glass beads in ACN prior to sample addition improved reproducibility and avoided dilution from aqueous bead slurries. Glass beads therefore offer clear

https://doi.org/10.1021/acs.analchem.1c04200
Anal. Chem. 2022, 94, 10320−10328

advantages over SP4-BF and may offer benefits for other protein precipitation approaches.

Where SP4 outperformed SP3, the use of centrifugation appears to have mitigated losses arising from dependence on effective magnetic capture of protein−bead aggregation. Aggregation-resistant proteins and fragile aggregates prone to mechanical disruption would risk removal with the supernatant and washes. This likely explains, alongside improved reproducibility, the greater recovery by SP4 (and cSP3) of hydrophobic and lower-solubility proteins—which exhibit a reduced propensity for organic solvent-induced aggregation.[34] Interestingly, some marginal losses to membrane proteins remained during cSP3 (Figure 2D-iii,E-iii), suggesting either superior glass bead binding of hydrophobic proteins or incomplete elution of hydrophobic peptides from CMMBs. The higher recovery of low-molecular-weight proteins by SP3 does suggest that carboxylate chemistry may facilitate the capture of some peptides which are less prone to precipitation.[30,32]

At high protein concentrations, SP4 and SP3 yielded consistent recovery across the majority of the proteome—adding to suggestions that protein precipitation is the primary mechanism of SP3.[8,13] Protein−protein and protein−CMMB aggregation both likely derive from highly similar electrostatic interactions of protein elements exposed by dehydration and denaturation. This may explain the paradoxical losses observed at higher protein inputs and concentrations for SP3[5,11] (Figures 1B and S1C) if protein−CMMB aggregation is outcompeted by protein−protein aggregation, resulting in particles that are not captured by magnetism. Conversely, at lower protein concentrations, where nucleation points are scarce, the rapid nature of denaturation-induced aggregation—often termed a protein "crash"—drives finer precipitate formation and tube-wall adhesion and perhaps explains the low yield observed for SP4-BF (Figure 1D). CMMBs therefore appear to alleviate the scarcity of protein−protein interaction sites at lower concentrations by providing additional electrostatic nucleation points, thereby expediting more stable precipitation. HILIC-type interactions may also play a role in this process. Although glass beads also ameliorated bead-free losses, their effect was less pronounced, perhaps due to the lack of additional electrostatic nucleation and reliance on hydrophobic interactions alone, which are weaker in nature and thus may proceed more slowly. Therefore, while protein precipitation appears to be the primary mechanism of protein capture for both SP3 and SP4, CMMB and GB physicochemical properties may offer some mechanistic divergence in the role they provide as nucleation points, driving initial aggregate capture more prevalently through electrostatic and hydrophobic interactions, respectively.

A precipitation mechanism also has implications for organic solvent concentration selection, where higher percentages offer greater denaturation. This was apparent among the consistently lower recovery of many proteins observed with the use of 50% ACN for both SP3 and cSP3 *vs* 80%, most notably for low-molecular-weight proteins. However, there was a marginal signature of higher global median protein yield (Figure 2C, also noted in Figure S1), likely arising from the lower and thus more concentrated aggregation reaction volume. This indicates a trade-off between the improved recovery of subsets of hydrophobic and low-molecular-weight proteins (80% ACN) and marginally higher global yields (50% ACN). The role of protein precipitation in SP3 also suggests that ionic strength, like with SP4, should be carefully considered during aggregation.[25]

SP4-GB broadly matched S-Trap, offering marginally higher yields (Figures 2C,D-iv and S9)—perhaps resulting from losses on the additional surfaces presented by the S-Trap protocol. S-Trap had lower variability for label-free samples (Figure S9) but not for the TMT samples (Figure 2-iv). Notably, SP4 eschews the specialist devices, multiple elution steps, peptide concentration steps, multiple vessels, and buffer restrictions of S-Trap. Importantly, our presentation of a common mechanistic bridge between SP3 and other protein precipitation-based methods such as S-Trap, ProTrap-XG, and filter-aided SPEED offers several potential avenues for further optimization and cross-adaptation of existing best practices.

Alongside limitations at low protein concentrations and the loss of some low-molecular-weight proteins,[30,32] SP4 does not benefit from certain advantages offered by CMMBs, *e.g.*, the options to enrich peptides or adapt for high throughput and automation[8,14−16] (although we note that SP4 was compatible with lower centrifugation speeds more typically employed for 96-well plates (Figure S5D)).

SP4 undoubtedly has the potential for further optimization. For example, the precipitation step could be enhanced by cold temperatures, carefully titrated ACN concentrations, and longer centrifugation at slower speeds. The trade-off between a denser aggregate pellet and the ease of resuspension for trypsin accessibility may be worthy of further exploration (Figure S5D), although Lys-C, rapid digestion buffers, and higher digestions temperatures appear to be effective solutions (Figures 2 and 3D). The type of bead is also worthy of exploration, such as size, material, and surface chemistry. Cheaper, non-magnetic carboxylate-modified beads used alongside centrifugation and washes, like cSP3, might offer benefits of both approaches.

CONCLUDING REMARKS

SP4 addresses key limitations of SP3 with the use of centrifugation and glass beads, providing a minimalistic, low-cost protein cleanup method that offers greater or equivalent protein yields when protein concentration and input are sufficient. SP4 is particularly applicable to the preparation of high-input samples (*e.g.*, for PTM preparations) and for biology labs with limited proteomics experience and preparation equipment. We provide further evidence that precipitation is the primary mechanism of SP3 cleanup and that CMMBs can be omitted from high-concentration protein capture in many applications. We hope these findings will extend options, improve understanding, and encourage further development of proteomics sample cleanup methods.

ASSOCIATED CONTENT

Supporting Information

The Supporting Information is available free of charge at https://pubs.acs.org/doi/10.1021/acs.analchem.1c04200.

Expanded results, analysis, optimization work, and additional exploratory experiments (Figures S1−S9); supporting methods; supporting methods for validation work; detailed step-by-step protocol for SP4-BF or SP4-GB sample preparation (SP4 protocol); detailed tables and summaries of the proteomics findings (Tables S1−S20) (PDF)

(XLSX)

https://doi.org/10.1021/acs.analchem.1c04200
Anal. Chem. 2022, 94, 10320−10328

AUTHOR INFORMATION

Corresponding Authors

Harvey E. Johnston − *Signalling Programme, The Babraham Institute, Cambridge CB22 3AT, United Kingdom;* orcid.org/0000-0001-7032-0227; Email: harvey.johnston@babraham.ac.uk

Rahul S. Samant − *Signalling Programme, The Babraham Institute, Cambridge CB22 3AT, United Kingdom;* Email: rahul.samant@babraham.ac.uk

Authors

Kranthikumar Yadav − *Mass Spectrometry Facility, The Babraham Institute, Cambridge CB22 3AT, United Kingdom*

Joanna M. Kirkpatrick − *Proteomics STP, The Francis Crick Institute, London NW1 1AT, United Kingdom;* orcid.org/0000-0001-9291-7294

George S. Biggs − *Proteomics STP, The Francis Crick Institute, London NW1 1AT, United Kingdom; GlaxoSmithKline, Stevenage SG1 2NY Hertfordshire,, United Kingdom*

David Oxley − *Mass Spectrometry Facility, The Babraham Institute, Cambridge CB22 3AT, United Kingdom*

Holger B. Kramer − *Medical Research Council London Institute of Medical Sciences, Imperial College London, London W12 0NN, United Kingdom*

Complete contact information is available at: https://pubs.acs.org/10.1021/acs.analchem.1c04200

Author Contributions

Conceptualization, data curation, formal analysis, methodology, visualization, investigation: H.E.J.; Writing − original draft: H.E.J., R.S.S.; Funding acquisition: R.S.S.; Resources: K.Y., J.K., G.B., D.O., and H.K.; Supervision: H.K., R.S.S.; Validation: K.Y., J.K., G.B., and H.K.; Writing−review and editing: H.E.J., K.Y., J.K., G.B., D.O., H.K., and R.S.S.

Notes

The authors declare no competing financial interest.

ACKNOWLEDGMENTS

The authors would like to thank Richard Kay for useful discussions about peptidomics methods, John Timms, who helped to support early work that inspired this study, Angus Lamond and Sara ten Have for their kind gift of FFPE tissue samples, Ian McGough for providing *Drosophila* lysate, Stephen Chetwynd and Julia Chu for their assistance with generating mouse whole tissue lysates, and Andrea Lopez for assistance with access to Proteome Discoverer. H.E.J. and R.S.S. are funded by Institute Strategic Programme Grant BB/P013384/1 from the BBSRC.

REFERENCES

(1) Yates, J. R.; Ruse, C. I.; Nakorchevsky, A. *Annu. Rev. Biomed. Eng.* **2009**, *11*, 49−79.

(2) Loo, R. R. O.; Dales, N.; Andrews, P. C. *Protein Sci.* **1994**, *3*, 1975−1983.

(3) Kulak, N. A.; Pichler, G.; Paron, I.; Nagaraj, N.; Mann, M. *Nat. Methods* **2014**, *11*, 319−324.

(4) Wiśniewski, J. R.; Zougman, A.; Nagaraj, N.; Mann, M. *Nat. Methods* **2009**, *6*, 359−362.

(5) Sielaff, M.; Kuharev, J.; Bohn, T.; Hahlbrock, J.; Bopp, T.; Tenzer, S.; Distler, U. *J. Proteome Res.* **2017**, *16*, 4060−4072.

(6) Zeller, M.; Brown, E. K.; Bouvier, E. S.; Konig, S. *J. Biomol. Tech* **2002**, *13*, 1−4.

(7) Tubaon, R. M.; Haddad, P. R.; Quirino, J. P. *Proteomics* **2017**, *17*, No. 1700011.

(8) Hughes, C. S.; Foehr, S.; Garfield, D. A.; Furlong, E. E.; Steinmetz, L. M.; Krijgsveld, J. *Mol. Syst. Biol.* **2014**, *10*, 757.

(9) Hughes, C. S.; Moggridge, S.; Muller, T.; Sorensen, P. H.; Morin, G. B.; Krijgsveld, J. *Nat. Protoc.* **2019**, *14*, 68−85.

(10) Moggridge, S.; Sorensen, P. H.; Morin, G. B.; Hughes, C. S. *J. Proteome Res.* **2018**, *17*, 1730−1740.

(11) Dagley, L. F.; Infusini, G.; Larsen, R. H.; Sandow, J. J.; Webb, A. I. *J. Proteome Res.* **2019**, *18*, 2915−2924.

(12) Hughes, C. S.; McConechy, M. K.; Cochrane, D. R.; Nazeran, T.; Karnezis, A. N.; Huntsman, D. G.; Morin, G. B. *Sci. Rep.* **2016**, *6*, No. 34949.

(13) Batth, T. S.; Tollenaere, M. A. X.; Ruther, P.; Gonzalez-Franquesa, A.; Prabhakar, B. S.; Bekker-Jensen, S.; Deshmukh, A. S.; Olsen, J. V. *Mol. Cell. Proteomics* **2019**, *18*, 1027−1035.

(14) Leutert, M.; Rodriguez-Mias, R. A.; Fukuda, N. K.; Villen, J. *Mol. Syst. Biol.* **2019**, *15*, No. e9021.

(15) Müller, T.; Kalxdorf, M.; Longuespee, R.; Kazdal, D. N.; Stenzinger, A.; Krijgsveld, J. *Mol. Syst. Biol.* **2020**, *16*, No. e9111.

(16) Deng, W.; Sha, J.; Plath, K.; Wohlschlegel, J. A. *Mol. Cell. Proteomics* **2021**, No. 100039.

(17) Fic, E.; Kedracka-Krok, S.; Jankowska, U.; Pirog, A.; Dziedzicka-Wasylewska, M. *Electrophoresis* **2010**, *31*, 3573−3579.

(18) Jiang, L.; He, L.; Fountoulakis, M. *J. Chromatogr. A* **2004**, *1023*, 317−320.

(19) Wessel, D.; Flugge, U. I. *Anal. Biochem.* **1984**, *138*, 141−143.

(20) Simpson, D. M.; Beynon, R. J. *J. Proteome Res.* **2010**, *9*, 444−450.

(21) Güray, M. Z.; Zheng, S.; Doucette, A. A. *J. Proteome Res.* **2017**, *16*, 889−897.

(22) Zougman, A.; Selby, P. J.; Banks, R. E. *Proteomics* **2014**, *14*, 1006−1000.

(23) Doellinger, J.; Schneider, A.; Hoeller, M.; Lasch, P. *Mol. Cell. Proteomics* **2020**, *19*, 209−222.

(24) Nickerson, J. L.; Baghalabadi, V.; Dang, Z.; Miller, V. A.; Little, S. L.; Doucette, A. A. *J. Visualized Exp.* **2022**, No. 180.

(25) Nickerson, J. L.; Doucette, A. A. *J. Proteome Res.* **2020**, *19*, 2035−2042.

(26) Perez-Riverol, Y.; Csordas, A.; Bai, J.; Bernal-Llinares, M.; Hewapathirana, S.; Kundu, D. J.; Inuganti, A.; Griss, J.; Mayer, G.; Eisenacher, M.; Perez, E.; Uszkoreit, J.; Pfeuffer, J.; Sachsenberg, T.; Yilmaz, S.; Tiwary, S.; Cox, J.; Audain, E.; Walzer, M.; Jarnuczak, A. F.; Ternent, T.; Brazma, A.; Vizcaino, J. A. *Nucleic Acids Res.* **2019**, *47*, D442−D450.

(27) Sormanni, P.; Aprile, F. A.; Vendruscolo, M. *J. Mol. Biol.* **2015**, *427*, 478−490.

(28) Schmidt, T.; Frishman, D. *BMC Bioinf.* **2006**, *7*, No. 331.

(29) Kozlowski, L. P. *Nucleic Acids Res.* **2017**, *45*, D1112−D1116.

(30) Parker, B. L.; Burchfield, J. G.; Clayton, D.; Geddes, T. A.; Payne, R. J.; Kiens, B.; Wojtaszewski, J. F. P.; Richter, E. A.; James, D. E. *Mol. Cell. Proteomics* **2017**, *16*, 2055−2068.

(31) Polson, C.; Sarkar, P.; Incledon, B.; Raguvaran, V.; Grant, R. *J. Chromatogr. B.* **2003**, *785*, 263−275.

(32) Kay, R. G.; Challis, B. G.; Casey, R. T.; Roberts, G. P.; Meek, C. L.; Reimann, F.; Gribble, F. M. *Rapid Commun. Mass Spectrom.* **2018**, *32*, 1414−1424.

(33) Bruce, S. J.; Tavazzi, I.; Parisod, V.; Rezzi, S.; Kochhar, S.; Guy, P. A. *Anal. Chem.* **2009**, *81*, 3285−3296.

(34) Srivastava, O. P.; Srivastava, K. *Curr. Eye Res.* **1998**, *17*, 1074−1081.

Supporting Information

Solvent Precipitation SP3 (SP4) enhances recovery for proteomics sample preparation without magnetic beads

AUTHORS
Harvey E. Johnston[1]*, Kranthikumar Yadav[2], Joanna M. Kirkpatrick[3], George S. Biggs[3,4], David Oxley[2], Holger B. Kramer[5], Rahul S. Samant[1]*

1. Signalling Programme, The Babraham Institute, Cambridge, CB22 3AT, United Kingdom
2. Mass Spectrometry Facility, The Babraham Institute, Cambridge, CB22 3AT, United Kingdom
3. Proteomics STP, The Francis Crick Institute, London, NW1 1AT, United Kingdom
4. GlaxoSmithKline, Gunnels Wood Road, Stevenage, Hertfordshire, SG1 2NY, United Kingdom
5. Medical Research Council London Institute of Medical Sciences, Imperial College London, Hammersmith Hospital, London, W12 0NN, United Kingdom

*Corresponding authors: harvey.johnston@babraham.ac.uk; rahul.samant@babraham.ac.uk

Additional information:

Table S1 – S20 (.xlsx spreadsheet) Detailed tables and summaries of the proteomics findings. All values are unnormalized to demonstrate technical effects on recovery.

Table S1. Key measures of proteome quality outputs from label-free comparisons of SP3 with bead-free (BF) and glass bead (GB) SP4 (Summarizing **Tables S2 – S8** and illustrated in **Fig 1B and S2**)

Table S2. 1 *µ*g (of protein) SP3 *vs* SP4-BF *vs* SP4-GB preparation proteomics (**Fig 1B**)

Table S3. 10 *µ*g (of protein) SP3 *vs* SP4-BF *vs* SP4-GB preparation proteomics (**Fig 1B**)

Table S4. 100 *µ*g (of protein) SP3 *vs* SP4-BF *vs* SP4-GB preparation proteomics (**Fig 1B**)

Table S5. 500 *µ*g (of protein) SP3 *vs* SP4-BF *vs* SP4-GB preparation proteomics (**Fig 1B**)

Table S6. 5000 *µ*g (of protein) SP3 *vs* SP4-BF *vs* SP4-GB preparation proteomics (**Fig 1B**)

Table S7. 10 *µ*g optimization experiments, exploring centrifugation speed, bead:protein ratio, ACN concentration, use of centrifugation with SP3 beads (cSP3), and the application of the SPEED method, summarized in **Fig S1** and **S5**

Table S8. 500 *µ*g prepared using 8 M urea as the lysis buffer, requiring the dilution of samples to 2 M urea prior to SP3/SP4, summarized in **Fig S5**

Table S9. TMT 6-plex of 100 *µ*g processed by SP3 (*n* = 2), SP4-BF (*n* = 2), and SP4-GB (*n* = 2)

Table S10. TMT 6-plex of 100 *µ*g processed by SP4-GB (*n* = 2), SP3 with 80% ACN (*n* = 2), and SP3 with 50% ACN (*n* = 2)

Table S11. TMT 6-plex of 100 *µ*g processed by SP4-GB (*n* = 2), centrifugal SP3 (cSP3) with 80% ACN (*n* = 2), and cSP3 with 50% ACN (*n* = 2)

Table S12. TMT 6-plex of 100 *µ*g processed by SP4-GB (*n* = 2), S-Trap (*n* = 2), and 0.2 *µ*m spin filters (*n* = 2)

Table S13. 100 *µ*g processed by SP4-GB (*n* = 4), S-Trap (*n* = 4), and 0.2 *µ*m spin filters (*n* = 4) by LFQ

Table S14. 1 *µ*g processed at a protein concentration of 0.025 *µ*g/*µ*L by SP3 *vs* SP4-BF *vs* SP4-GB preparation proteomics (**Fig 1D**)

Table S15. 500 *µ*g SP3, SP4-BF, and SP4-GB using acetone (ACT) and acetonitrile (ACN), summarized in **Fig S5**

Table S16. 20 *µ*g mouse heart lysate processed by SP3 and SP4-GB (*n* = 3)

Table S17. 20 *µ*g mouse lung lysate processed by SP3 and SP4-GB (*n* = 3)

Table S18. 20 *µ*g mouse liver FFPE tissue lysate processed by SP3 and SP4-GB (*n* = 3)

Table S19. 20 *µ*g mouse brain FFPE tissue lysate processed by SP3 and SP4-GB (*n* = 3)

Table S20. 20 *µ*g whole *Drosophila* homogenate processed by SP3 and SP4-GB (*n* = 3)

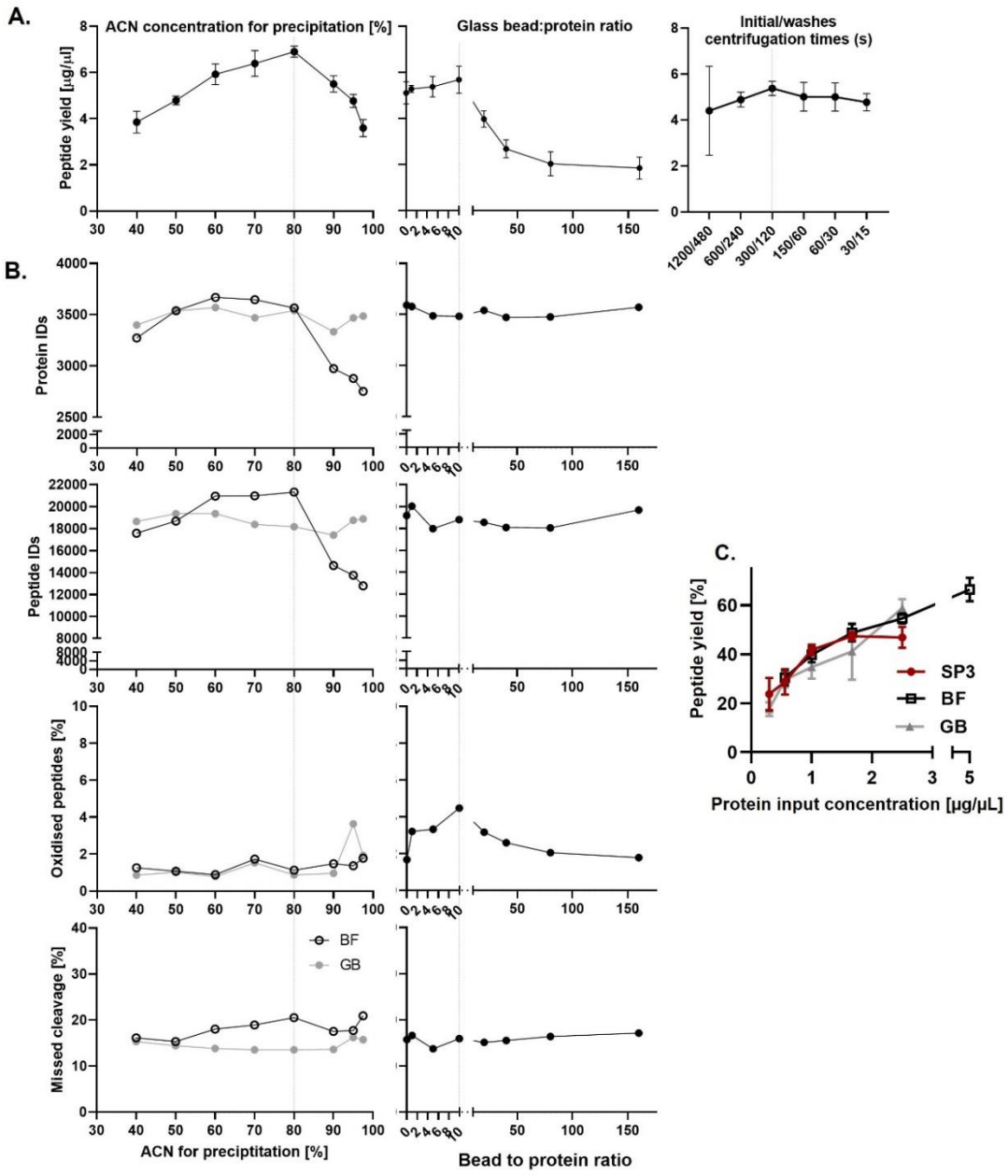

Figure S1. **Evaluation of a range of SP4-related variables by peptide quantitation assay (*n* = 4) and proteomics analysis. A.** 10 *µ*g of protein was processed by SP4 varying the initial and post-wash precipitate capture centrifugation times, the glass bead to protein ratio, and the total final percentage of ACN in the precipitation step. The digests were measured by peptide quantitation assay. **B.** For proteomics analyses, 10 *µ*g SP4 sample preparations were evaluated varying bead input and ACN concentration with 100 ng equivalent of peptides analysed by LC-MS. Other variables were kept at either 300/120 s capture/wash centrifugation steps, 10:1 glass bead to protein ratio and 80% ACN. **C.** 50 *µ*g of protein was processed by SP3, SP4-BF and SP4-GB methods across a range of protein concentrations representative of that of the final volume, including the volume from the bead suspension for SP3 and SP4-GB. It was therefore possible to evaluate SP4-BF at twice the protein concentration, with no bead addition required. The samples were subjected to SP3 and SP4 protocols, digested with trypsin in 20 mM ammonium bicarbonate (ABC) and the resulting peptides were measured by peptide assay.

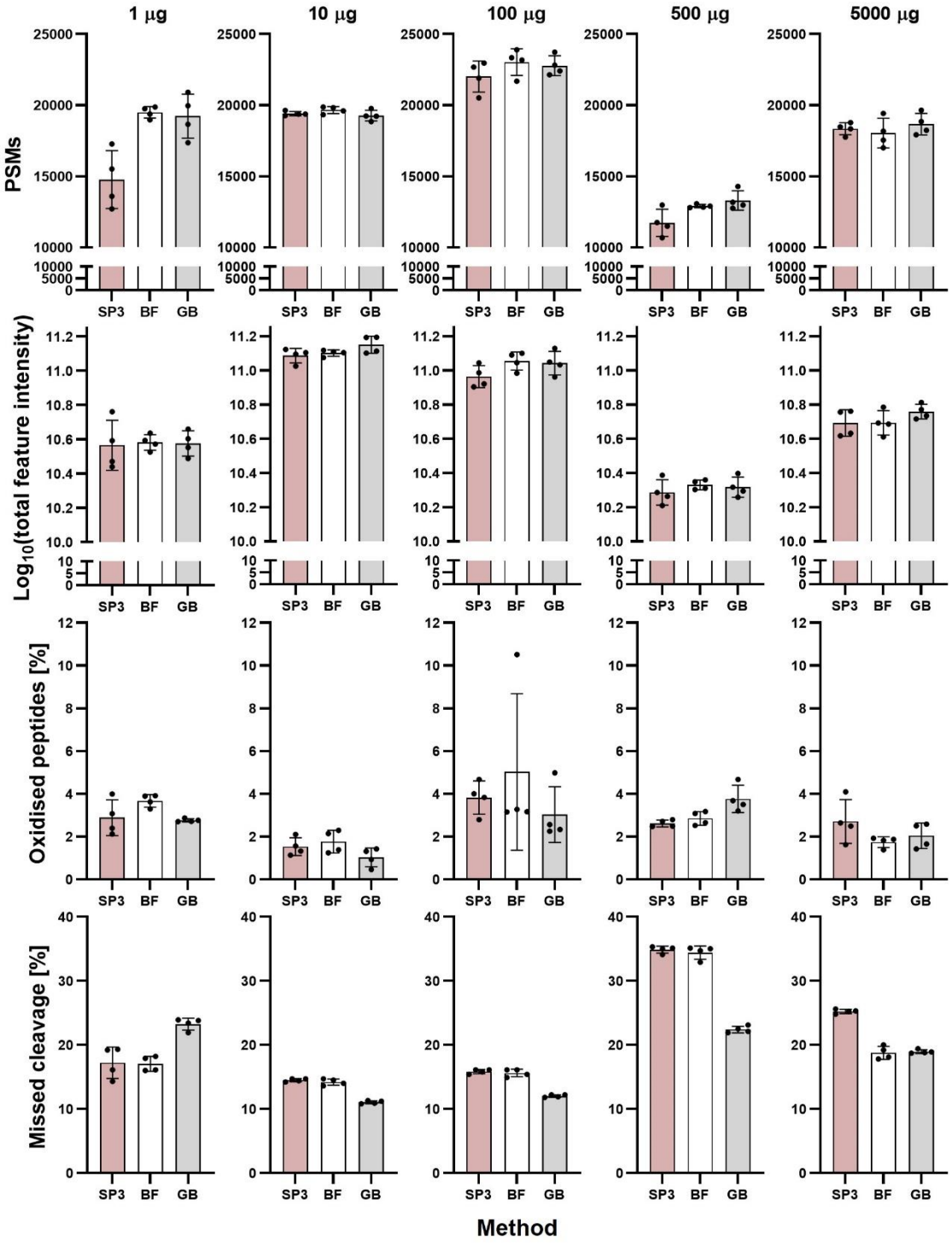

Figure S2. **Additional measure of proteome quality and protein recovery for the comparison of SP3 to SP4 with (GB) and without glass beads (bead-free, BF) across the range of evaluated protein inputs (see also Fig 1B).** PSM = peptide spectrum match.

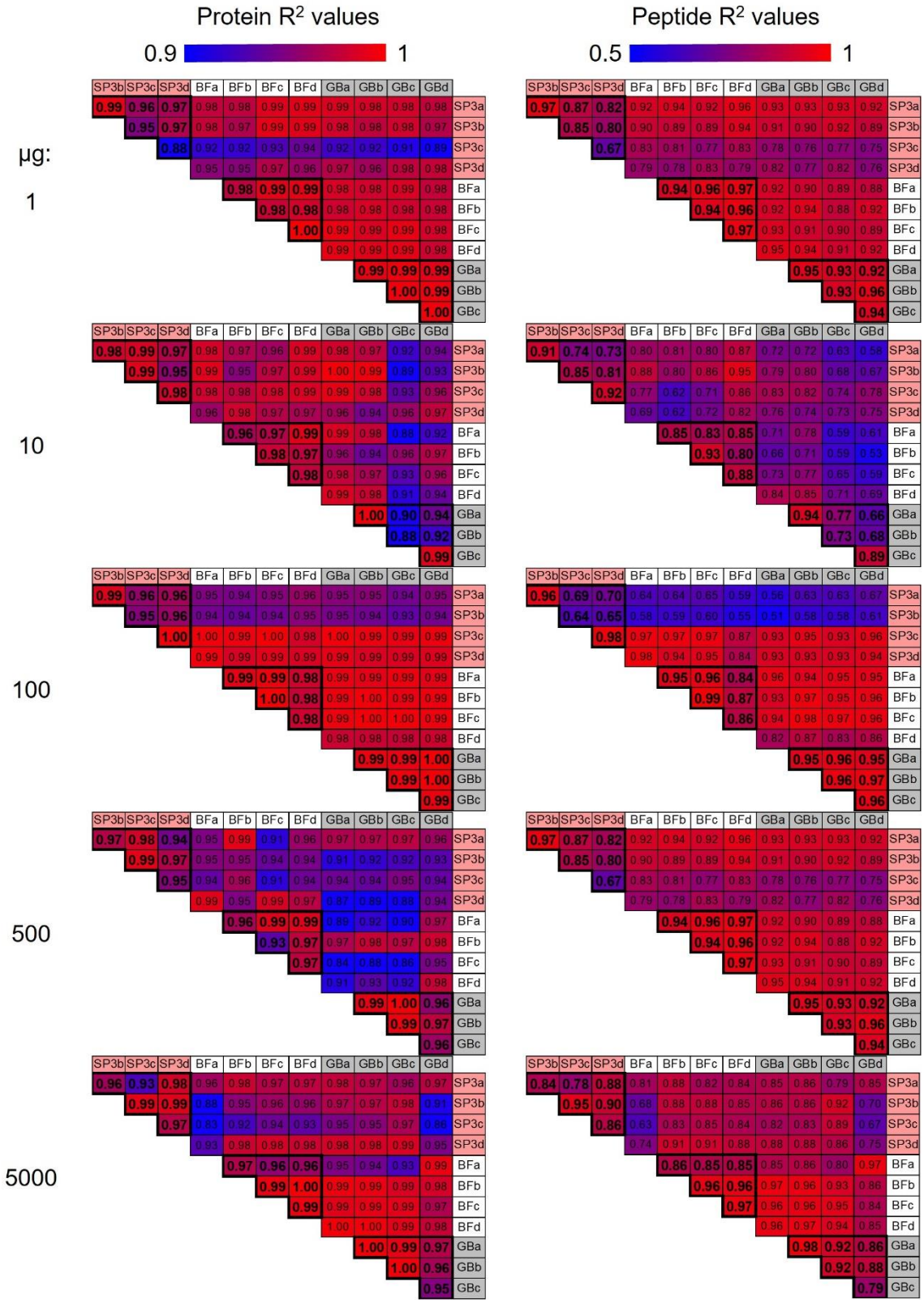

Figure S3. Protein and peptide LFQ R^2 values of recovery for SP3 to SP4, with (GB) and without glass beads (bead-free, BF), across the range of evaluated protein inputs (Fig 1B).

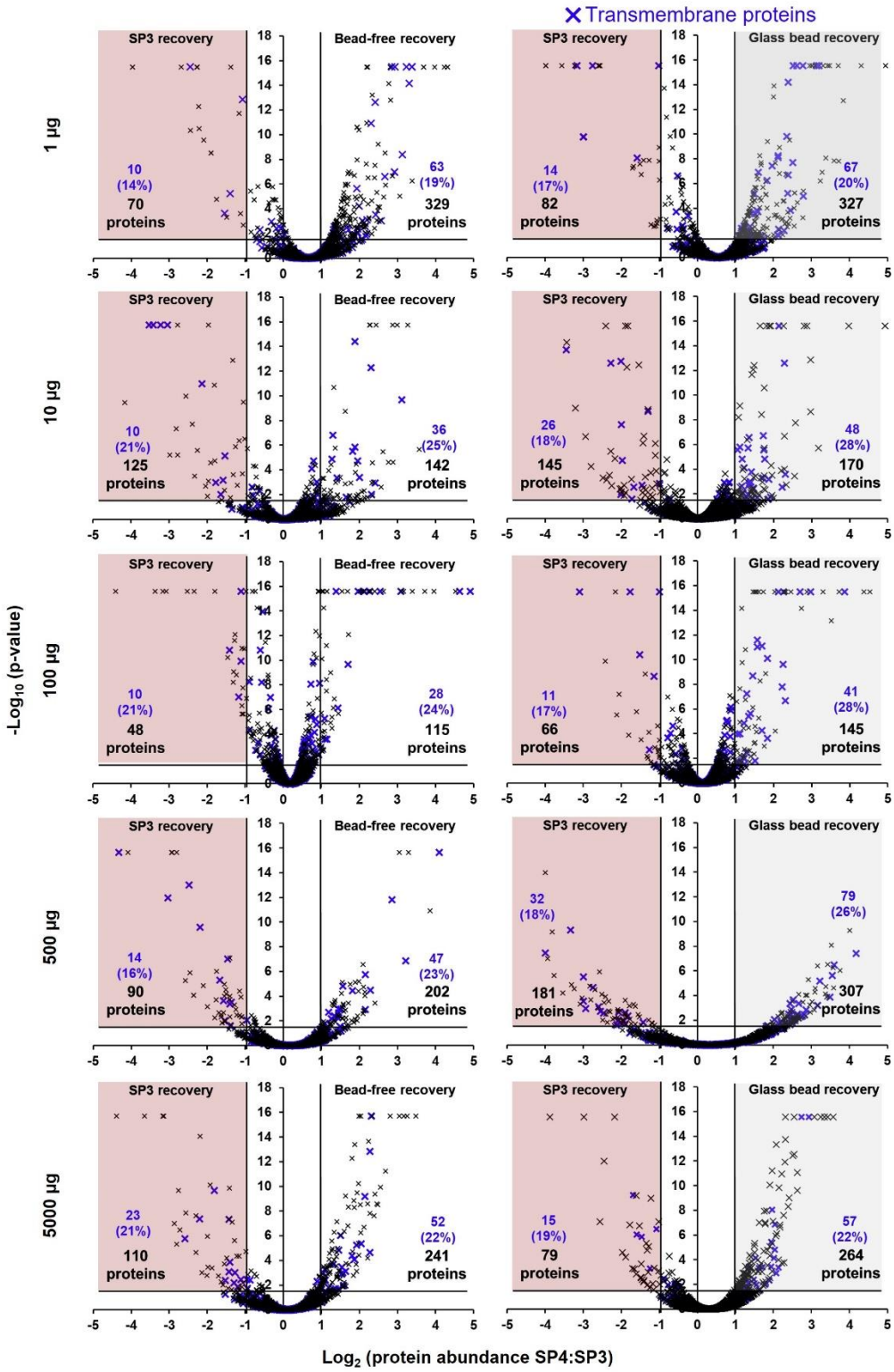

Figure S4. **Protein recovery observed to be significantly more effective by SP4 variants *vs* SP3, summarized in Fig 1B.** *p*-values determined by Proteome Discoverer with multiple-test adjusted *t*-test. Blue crosses and numbers denote transmembrane proteins, with the proportion of the significantly differentially recovery proteins ($log_2(FC) > 1$, $p < 0.05$) annotated as transmembrane proteins in brackets.

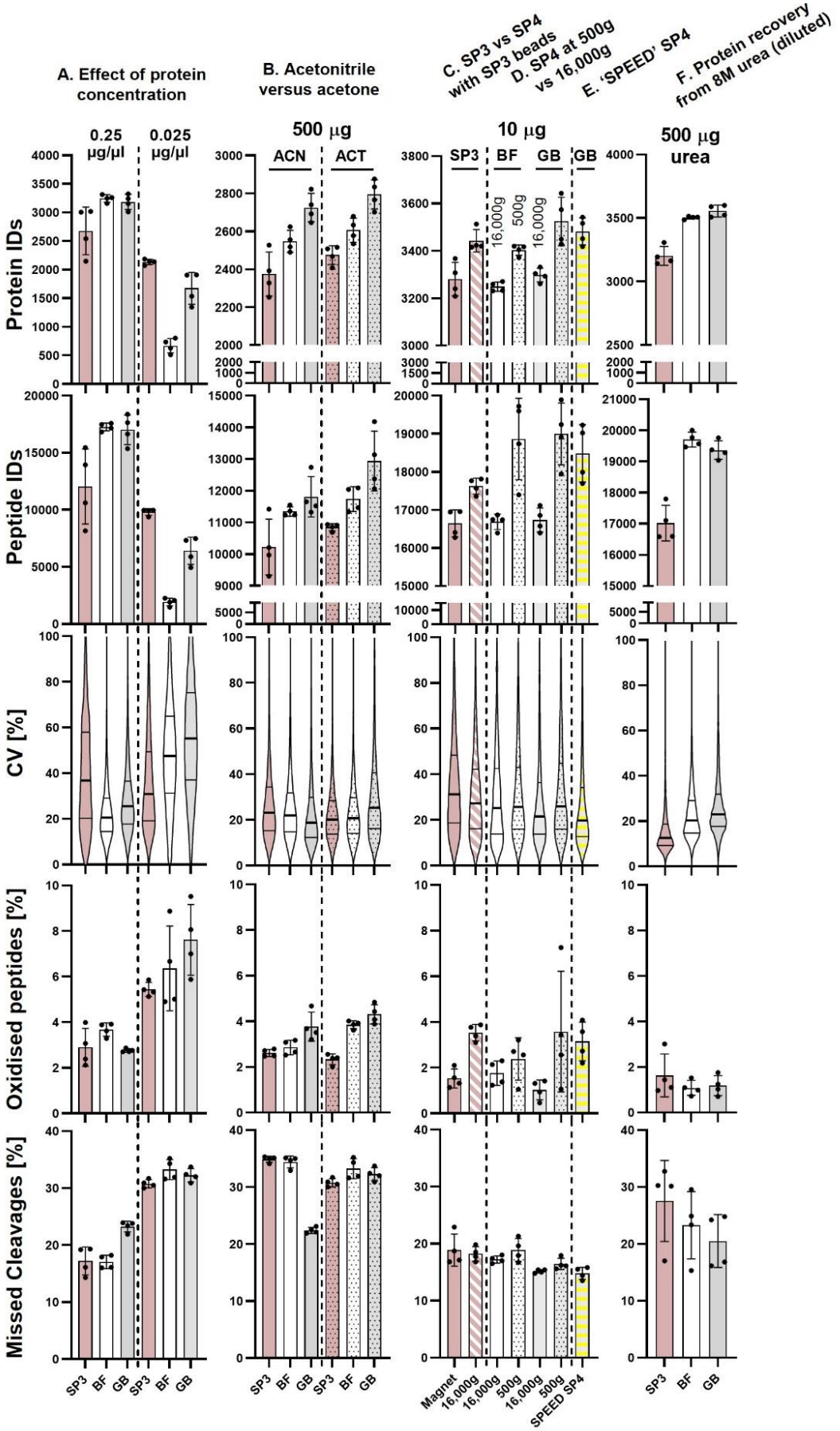
A. Effect of protein concentration
B. Acetonitrile versus acetone
C. SP3 vs SP4 with SP3 beads
D. SP4 at 500g vs 16,000g
E. 'SPEED' SP4
F. Protein recovery from 8M urea (diluted)
0.25 µg/µl
0.025 µg/µl
500 µg
ACN
ACT
10 µg
SP3
BF
GB
16,000g
500g
500 µg urea
Protein IDs
Peptide IDs
CV [%]
Oxidised peptides [%]
Missed Cleavages [%]
Magnet
SPEED SP4

Figure S5. **Additional experiments exploring the mechanism and potential of bead-free (BF) and glass bead (GB) SP4.** Protein numbers, peptide numbers, peptide CVs, oxidised peptides, and missed cleavage rates among peptide spectrum matches are detailed for the 4 procedural replicates. **A.** 1 *µ*g SP3 and SP4 preparations were conducted using two initial protein concentrations: 250 ng/*µ*L (1 *µ*g in 4 *µ*L volume, including beads) and 25 ng/*µ*L (1 *µ*g in 20 *µ*L volume, including beads). **B.** 500 *µ*g SP3 or SP4 preparations were conducted using acetonitrile (ACN) or acetone (ACT) as the denaturing solvent. **C.** SP3 was compared with SP4 using SP3 carboxylate magnetic beads to confirm that centrifugation recovered more protein than the use of a magnet. **D.** BF and GB SP4 variants were tested at 500*g* (vs. 16,000*g* adopted in all other experiments) for the potential to expand their compatibility with larger volume and plate-based preparations. **E.** Cells were lysed by 'SPEED' (Sample Preparation by Easy Extraction and Digestion) method using 100% TFA and neutralised with Tris base before being subjected to SP4 with the inclusion of glass beads. **F.** 500 *µ*g of protein was processed by SP3 to SP4 using 8 M urea as the lysis buffer, across a range of measures of protein recovery and proteome quality. Lysate was diluted to 2 M urea prior to addition of beads and ACN.

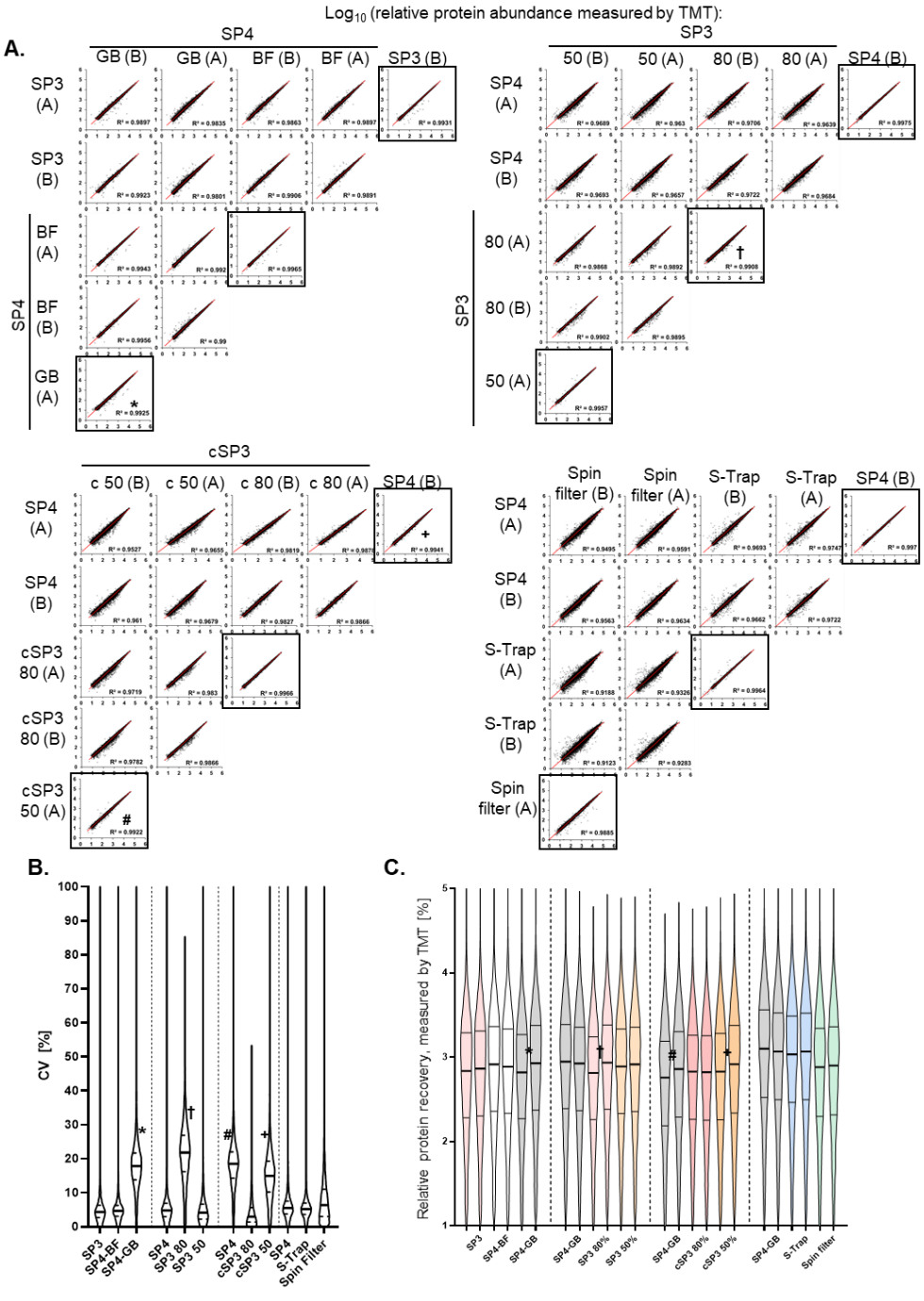

Figure S6. Measures of quantitative proteome reproducibility for comparison of SP3 and SP4 using TMT 6-plex, summarized in Figure 2. Correlations between TMT-measured protein abundances for sample preparations and method replicates (**A.**) and coefficients of variation (CV) % (**B.**) and total protein abundance value distributions (**C.**). Data are not normalized to enable full assessment of technical variations (correlation is therefore a better measure of consistency in this instance). Boxes denote the direct correlations between methodological replicates. Those replicates with higher CV% are footnoted *, †, #, and + to their corresponding R^2 values, demonstrating that, despite differential total recovery, this was consistent across the whole proteome and did not indicate differential protein loss, with no reduction of relative correlation.

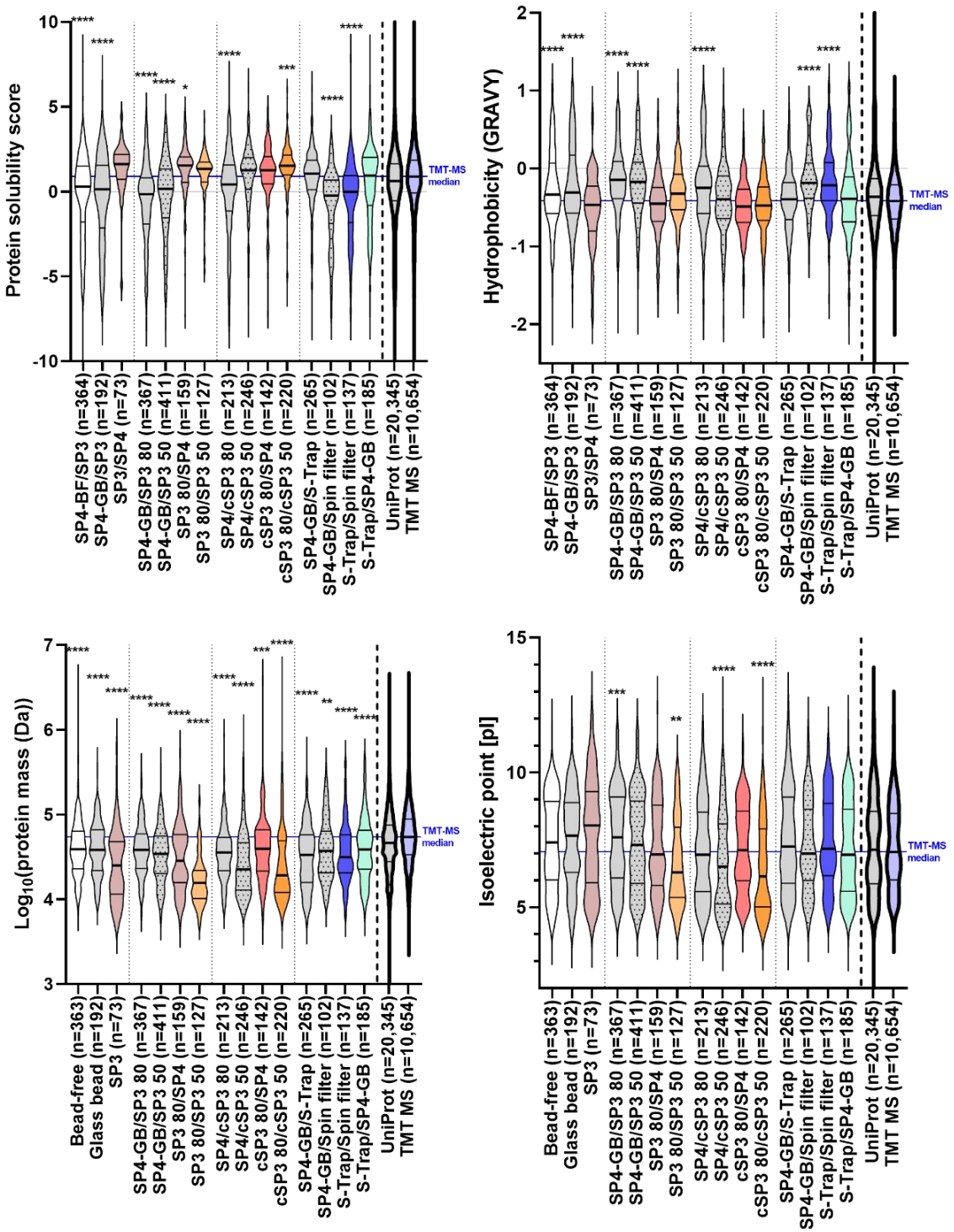

Figure S7. Frequency distributions of physical properties among proteins with significantly greater recovery (defined in Fig 2D). Both the human UniProt Swissprot (grey) and the MS-derived TMT (blue) proteomes are displayed as percentage frequency backgrounds. ANOVA followed by Dunnett's multiple comparisons test, compared to the TMT proteome-identified proteins, was used to assess significant deviation from an expected background distribution. Protein coefficients of variance distributions represented by violin plot (thick line–median, thin lines–quartiles). *$p < 0.05$, **$p < 0.01$, ***$p < 0.001$, ****$p < 0.0001$, and ns–not significant.

Figure S8 – TMT i.

Functional annotation clustering: **Functional annotation terms:**

'Bead-free' proteins (n=364)

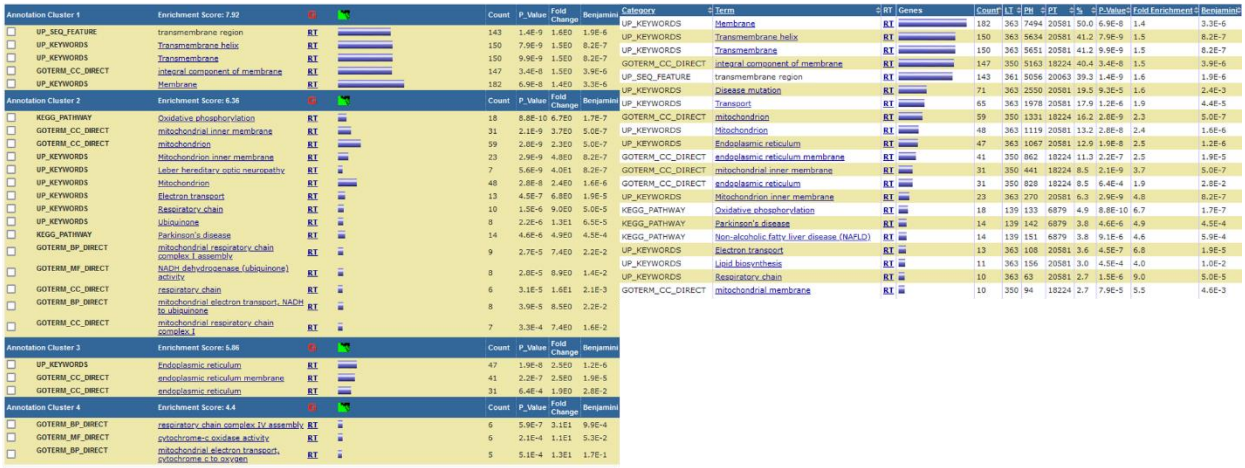

'Glass bead' proteins (n=193)

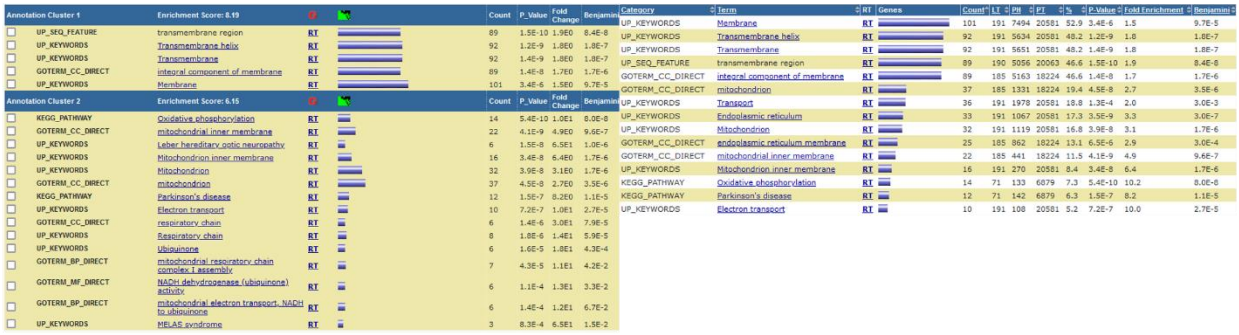

All SP4 proteins combined (n=400)

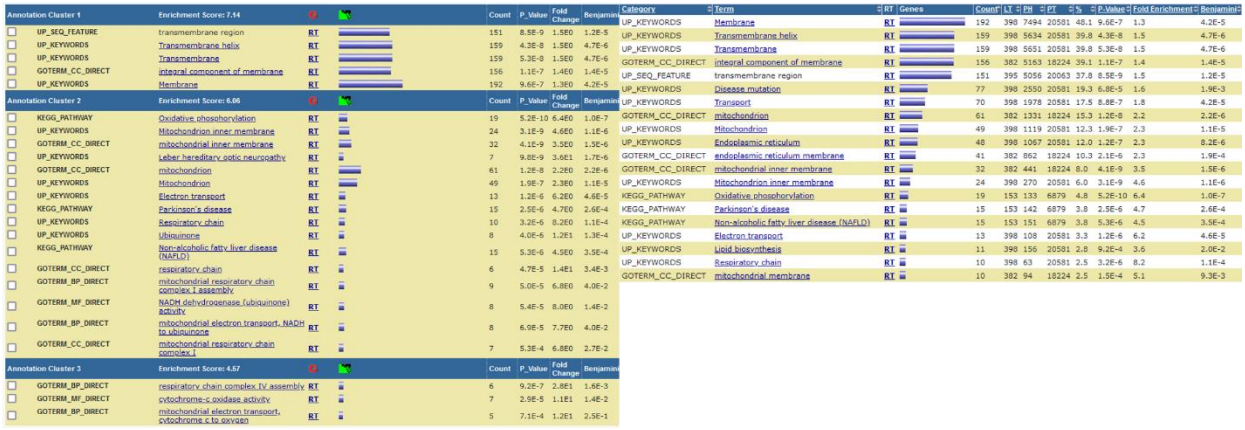

'SP3' proteins combined vs. BF+GB (n=73)

No significant clustered terms

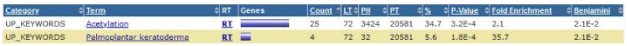

Figure S8 – TMT ii.

Functional annotation clustering: **Functional annotation terms:**

SP4-GB / SP3 80% ACN proteins (n=367):

Annotation Cluster 1	Enrichment Score: 9.96		Count	P_Value	Fold Change	Benjamini
GOTERM_CC_DIRECT	endoplasmic reticulum membrane	RT	56	1.0E-14	3.3E0	3.7E-12
UP_KEYWORDS	Endoplasmic reticulum	RT	57	2.7E-13	3.0E0	4.1E-11
GOTERM_CC_DIRECT	endoplasmic reticulum	RT	32	4.8E-4	2.0E0	1.6E-2
Annotation Cluster 2	**Enrichment Score: 9.21**		**Count**	**P_Value**	**Fold Change**	**Benjamini**
UP_KEYWORDS	Transmembrane	RT	159	4.2E-11	1.6E0	3.2E-9
UP_KEYWORDS	Transmembrane helix	RT	158	6.8E-11	1.6E0	4.1E-9
UP_SEQ_FEATURE	transmembrane region	RT	143	1.2E-9	1.6E0	9.7E-7
UP_KEYWORDS	Membrane	RT	189	2.1E-9	1.4E0	8.9E-8
GOTERM_CC_DIRECT	integral component of membrane	RT	152	1.3E-8	1.5E0	1.3E-6
Annotation Cluster 3	**Enrichment Score: 8.48**		**Count**	**P_Value**	**Fold Change**	**Benjamini**
GOTERM_CC_DIRECT	mitochondrial inner membrane	RT	33	2.3E-10	3.8E0	4.3E-8
UP_KEYWORDS	Mitochondrion inner membrane	RT	24	6.1E-10	5.0E0	3.0E-8
UP_KEYWORDS	Mitochondrion	RT	46	2.5E-7	2.3E0	6.9E-6
Annotation Cluster 4	**Enrichment Score: 5.86**		**Count**	**P_Value**	**Fold Change**	**Benjamini**
KEGG_PATHWAY	N-Glycan biosynthesis	RT	12	6.9E-9	1.1E1	1.2E-6
UP_KEYWORDS	Congenital disorder of glycosylation	RT	10	4.2E-8	1.3E1	1.6E-6
GOTERM_BP_DIRECT	dolichol-linked oligosaccharide biosynthetic process	RT	6	8.0E-6	2.0E1	2.7E-3

Category	Term	RT	Genes	Count	LT	PH	PT	%	P-Value	Fold Enrichment	Benjamini
GOTERM_CC_DIRECT	endoplasmic reticulum membrane	RT		56	360	862	18224	15.3	1.0E-14	3.3	3.7E-12
UP_KEYWORDS	Transport	RT		83	366	1978	20581	22.6	1.7E-13	2.4	4.1E-11
UP_KEYWORDS	Endoplasmic reticulum	RT		57	366	1067	20581	15.5	2.7E-13	3.0	4.1E-11
UP_KEYWORDS	Acetylation	RT		116	366	3424	20581	31.6	1.3E-12	1.9	1.3E-10
UP_KEYWORDS	Transmembrane	RT		159	366	5651	20581	43.3	4.2E-11	1.6	3.2E-9
UP_KEYWORDS	Transmembrane helix	RT		158	366	5634	20581	43.1	6.8E-11	1.6	4.1E-9
GOTERM_CC_DIRECT	mitochondrial inner membrane	RT		33	360	441	18224	9.0	2.3E-10	3.8	4.3E-8
UP_KEYWORDS	Mitochondrion inner membrane	RT		24	366	270	20581	6.5	6.1E-10	5.0	3.0E-8
UP_SEQ_FEATURE	transmembrane region	RT		143	360	5056	20063	39.0	1.2E-9	1.6	9.7E-7
UP_KEYWORDS	Membrane	RT		189	366	7494	20581	51.5	2.1E-9	1.4	8.9E-8
KEGG_PATHWAY	N-Glycan biosynthesis	RT		12	155	49	6879	3.3	6.9E-9	10.9	1.2E-6
GOTERM_CC_DIRECT	integral component of membrane	RT		152	360	5163	18224	41.4	1.3E-8	1.5	1.3E-6
GOTERM_CC_DIRECT	membrane	RT		82	360	2200	18224	22.3	1.4E-8	1.9	1.3E-6
UP_KEYWORDS	Congenital disorder of glycosylation	RT		10	366	42	20581	2.7	4.2E-8	13.4	1.6E-6
GOTERM_BP_DIRECT	rRNA processing	RT		20	338	214	16792	5.4	6.7E-8	4.6	8.9E-5
UP_KEYWORDS	ER-Golgi transport	RT		13	366	94	20581	3.5	1.0E-7	7.8	3.5E-6
INTERPRO	Small GTPase superfamily, ARF type	RT		9	354	32	18559	2.5	1.1E-7	14.7	5.7E-5
UP_KEYWORDS	Protein transport	RT		32	366	610	20581	8.7	1.7E-7	2.9	5.0E-6
INTERPRO	Small GTPase superfamily, ARF/SAR type	RT		9	354	34	18559	2.5	1.9E-7	13.9	5.7E-5
UP_KEYWORDS	Mitochondrion	RT		46	366	1119	20581	12.5	2.5E-7	2.3	6.9E-6

SP4-GB / SP3 50% ACN proteins (n=411):

Annotation Cluster 1	Enrichment Score: 11.74		Count	P_Value	Fold Change	Benjamini
UP_KEYWORDS	Mitochondrion inner membrane	RT	30	1.5E-13	5.6E0	1.6E-11
GOTERM_CC_DIRECT	mitochondrial inner membrane	RT	38	2.1E-12	4.0E0	4.1E-10
UP_KEYWORDS	Mitochondrion	RT	59	1.8E-11	2.7E0	1.1E-9
Annotation Cluster 2	**Enrichment Score: 8.06**		**Count**	**P_Value**	**Fold Change**	**Benjamini**
UP_KEYWORDS	Transmembrane	RT	170	5.8E-10	1.5E0	3.0E-8
UP_KEYWORDS	Transmembrane helix	RT	169	8.7E-10	1.5E0	3.8E-8
UP_KEYWORDS	Membrane	RT	205	1.0E-8	1.4E0	4.0E-7
UP_SEQ_FEATURE	transmembrane region	RT	151	4.7E-8	1.5E0	4.4E-5
GOTERM_CC_DIRECT	integral component of membrane	RT	160	2.1E-7	1.4E0	1.6E-5
Annotation Cluster 3	**Enrichment Score: 3.49**		**Count**	**P_Value**	**Fold Change**	**Benjamini**
KEGG_PATHWAY	N-Glycan biosynthesis	RT	11	1.2E-7	9.7E0	7.7E-6
GOTERM_CC_DIRECT	oligosaccharyltransferase complex	RT	6	1.1E-6	2.8E1	5.9E-5
UP_KEYWORDS	Congenital disorder of glycosylation	RT	9	1.5E-6	1.1E1	4.1E-5
GOTERM_MF_DIRECT	dolichyl-diphosphooligosaccharide-protein glycotransferase activity	RT	5	2.3E-5	2.6E1	1.2E-2
GOTERM_BP_DIRECT	protein N-linked glycosylation via asparagine	RT	8	2.6E-5	8.9E0	3.5E-2

Category	Term	RT	Genes	Count	LT	PH	PT	%	P-Value	Fold Enrichment	Benjamini
UP_KEYWORDS	Transport	RT		99	409	1978	20581	24.1	4.3E-18	2.5	9.6E-16
UP_KEYWORDS	Acetylation	RT		139	409	3424	20581	33.8	6.2E-18	2.0	9.0E-16
GOTERM_CC_DIRECT	endoplasmic reticulum membrane	RT		60	397	862	18224	14.6	3.8E-15	3.2	1.4E-12
UP_KEYWORDS	Mitochondrion inner membrane	RT		30	409	270	20581	7.3	1.5E-13	5.6	1.6E-11
UP_KEYWORDS	Endoplasmic reticulum	RT		60	409	1067	20581	14.6	8.4E-13	2.8	6.3E-11
GOTERM_CC_DIRECT	mitochondrial inner membrane	RT		38	397	441	18224	9.2	2.1E-12	4.0	4.1E-10
UP_KEYWORDS	Mitochondrion	RT		59	409	1119	20581	14.4	1.8E-11	2.7	1.1E-9
UP_KEYWORDS	Transmembrane	RT		170	409	3651	20581	41.4	5.8E-10	1.5	3.0E-8
UP_KEYWORDS	Transmembrane helix	RT		169	409	3634	20581	41.1	8.7E-10	1.5	3.8E-8
GOTERM_CC_DIRECT	mitochondrion	RT		65	397	1331	18224	15.8	1.4E-9	2.2	1.7E-7
KEGG_PATHWAY	Metabolic pathways	RT		59	160	1219	6879	14.4	9.5E-9	2.1	1.8E-6
UP_KEYWORDS	Membrane	RT		205	409	7494	20581	49.9	1.0E-8	1.4	4.0E-7
UP_KEYWORDS	Protein transport	RT		36	409	610	20581	8.8	2.1E-8	3.0	7.1E-7
GOTERM_CC_DIRECT	membrane	RT		87	397	2200	18224	21.2	3.3E-8	1.8	3.1E-6
UP_SEQ_FEATURE	transmembrane region	RT		151	404	5056	20063	36.7	4.7E-8	1.5	4.4E-5
KEGG_PATHWAY	Oxidative phosphorylation	RT		17	160	133	6879	4.1	5.4E-8	5.5	5.0E-6
KEGG_PATHWAY	N-Glycan biosynthesis	RT		11	160	49	6879	2.7	1.2E-7	9.7	7.7E-6
GOTERM_CC_DIRECT	integral component of membrane	RT		160	397	5163	18224	38.9	2.1E-7	1.4	1.6E-5
UP_KEYWORDS	ER-Golgi transport	RT		13	409	94	20581	3.2	3.5E-7	7.0	1.1E-5
GOTERM_CC_DIRECT	extracellular exosome	RT		99	397	2811	18224	24.1	7.4E-7	1.6	4.7E-5

SP3 (80+50 % ACN) / SP4-GB proteins (n=185, combined):

Annotation Cluster 1	Enrichment Score: 2.78		Count	P_Value	Fold Change	Benjamini
UP_SEQ_FEATURE	short sequence motif:Twin CX3C motif	RT	4	1.4E-5	7.3E1	7.5E-3
INTERPRO	Tim10/DDP family zinc finger	RT	4	1.5E-5	7.2E1	5.2E-3
GOTERM_CC_DIRECT	mitochondrial intermembrane space	RT	7	5.4E-5	1.0E1	6.3E-3
GOTERM_CC_DIRECT	mitochondrial intermembrane space protein transporter complex	RT	3	7.9E-4	6.6E1	2.6E-2
Annotation Cluster 2	**Enrichment Score: 2.22**		**Count**	**P_Value**	**Fold Change**	**Benjamini**
GOTERM_CC_DIRECT	mitochondrial inner membrane	RT	16	1.1E-5	4.0E0	2.6E-3
KEGG_PATHWAY	Oxidative phosphorylation	RT	8	2.1E-4	6.4E0	3.3E-2
UP_KEYWORDS	Mitochondrion inner membrane	RT	10	6.9E-4	4.2E0	2.6E-2

Category	Term	RT	Genes	Count	LT	PH	PT	%	P-Value	Fold Enrichment	Benjamini
UP_KEYWORDS	Acetylation	RT		69	183	3424	20581	37.3	1.3E-11	2.3	2.9E-9
GOTERM_MF_DIRECT	protein binding	RT		114	159	8785	16681	61.6	4.1E-7	1.4	1.2E-4
UP_KEYWORDS	Mitochondrion	RT		29	183	1119	20581	15.7	6.1E-7	2.9	6.8E-5
GOTERM_CC_DIRECT	mitochondrial inner membrane	RT		16	165	441	18224	8.6	1.1E-5	4.0	2.6E-3
UP_SEQ_FEATURE	short sequence motif:Twin CX3C motif	RT		4	182	6	20063	2.2	1.4E-5	73.5	7.5E-3
INTERPRO	Tim10/DDP family zinc finger	RT		4	171	6	18559	2.2	1.5E-5	72.4	3.2E-3
GOTERM_CC_DIRECT	mitochondrial intermembrane space	RT		7	165	74	18224	3.8	5.4E-5	10.4	6.3E-3
UP_KEYWORDS	Cytoplasm	RT		66	183	4816	20581	35.7	1.1E-4	1.5	8.5E-3
GOTERM_CC_DIRECT	mitochondrion	RT		27	165	1331	18224	14.6	1.4E-4	2.2	8.9E-3
GOTERM_CC_DIRECT	cytoplasm	RT		70	165	5222	18224	37.8	1.5E-4	1.5	8.9E-3
KEGG_PATHWAY	Oxidative phosphorylation	RT		8	65	133	6879	4.3	2.1E-4	6.4	3.3E-2
GOTERM_CC_DIRECT	mediator complex	RT		5	165	35	18224	2.7	2.7E-4	15.8	1.2E-2
UP_KEYWORDS	Activator	RT		17	183	661	20581	9.2	2.7E-4	2.9	1.5E-2
UP_KEYWORDS	Nucleus	RT		68	183	5244	20581	36.8	4.5E-4	1.5	2.0E-2
UP_KEYWORDS	Mitochondrion inner membrane	RT		10	183	270	20581	5.4	6.9E-4	4.2	2.6E-2
GOTERM_CC_DIRECT	nucleoplasm	RT		42	165	2784	18224	22.7	7.7E-4	1.7	2.6E-2
GOTERM_CC_DIRECT	mitochondrial intermembrane space protein transporter complex	RT		3	165	5	18224	1.6	7.9E-4	66.3	2.6E-2

SP3 80% ACN / SP3 50% ACN proteins (n=127)

Annotation Cluster 1	Enrichment Score: 6.37		Count	P_Value	Fold Change	Benjamini
UP_KEYWORDS	Mitochondrion	RT	31	3.7E-12	4.5E0	3.2E-10
UP_KEYWORDS	Mitochondrion inner membrane	RT	16	9.9E-11	9.7E0	5.7E-9
GOTERM_CC_DIRECT	mitochondrion	RT	31	8.3E-10	3.6E0	8.5E-8
GOTERM_CC_DIRECT	mitochondrial inner membrane	RT	18	3.2E-9	6.3E0	1.7E-7
KEGG_PATHWAY	Oxidative phosphorylation	RT	11	3.5E-9	1.4E1	2.6E-7
KEGG_PATHWAY	Huntington's disease	RT	10	1.4E-6	8.5E0	5.2E-5
KEGG_PATHWAY	Parkinson's disease	RT	8	1.7E-5	9.2E0	4.3E-4
UP_KEYWORDS	Transit peptide	RT	14	2.3E-5	4.3E0	6.8E-4
KEGG_PATHWAY	Alzheimer's disease	RT	8	5.1E-5	7.8E0	9.6E-4
UP_SEQ_FEATURE	transit peptide:Mitochondrion	RT	12	1.9E-4	4.0E0	2.7E-2
KEGG_PATHWAY	Metabolic pathways	RT	17	1.0E-3	2.3E0	1.5E-2
KEGG_PATHWAY	Non-alcoholic fatty liver disease (NAFLD)	RT	6	1.9E-3	6.5E0	2.4E-2
Annotation Cluster 2	**Enrichment Score: 4.13**		**Count**	**P_Value**	**Fold Change**	**Benjamini**
INTERPRO	Tim10/DDP family zinc finger	RT	6	4.4E-11	1.6E2	8.5E-9
UP_SEQ_FEATURE	short sequence motif:Twin CX3C motif	RT	6	4.8E-11	1.6E2	1.3E-8
GOTERM_CC_DIRECT	mitochondrial intermembrane space protein transporter complex	RT	5	8.0E-9	1.5E2	3.2E-7
GOTERM_BP_DIRECT	chaperone-mediated protein transport	RT	5	1.2E-7	9.5E1	6.0E-5
UP_KEYWORDS	Chaperone	RT	11	4.2E-7	8.9E0	1.8E-5
GOTERM_BP_DIRECT	protein targeting to mitochondrion	RT	6	2.5E-6	2.7E1	6.5E-4
UP_KEYWORDS	Translocation	RT	7	1.2E-5	1.4E1	4.2E-4
GOTERM_BP_DIRECT	protein import into mitochondrial inner membrane	RT	3	4.1E-4	9.2E1	7.1E-2

Category	Term	RT	Genes	Count	LT	PH	PT	%	P-Value	Fold Enrichment	Benjamini
UP_KEYWORDS	Acetylation	RT		60	126	3424	20581	47.2	1.6E-15	2.9	2.8E-13
UP_KEYWORDS	Mitochondrion	RT		31	126	1119	20581	24.4	3.7E-12	4.5	3.2E-10
INTERPRO	Tim10/DDP family zinc finger	RT		6	113	6	18559	4.7	4.4E-11	164.2	8.5E-9
UP_SEQ_FEATURE	short sequence motif:Twin CX3C motif	RT		6	124	6	20063	4.7	4.8E-11	161.8	1.3E-8
UP_KEYWORDS	Mitochondrion inner membrane	RT		16	126	270	20581	12.6	9.9E-11	9.7	5.7E-9
GOTERM_CC_DIRECT	mitochondrion	RT		31	118	1331	18224	24.4	8.3E-10	3.6	8.5E-8
GOTERM_CC_DIRECT	mitochondrial intermembrane space	RT		10	118	74	18224	7.9	1.1E-9	20.9	8.5E-8
GOTERM_CC_DIRECT	mitochondrial inner membrane	RT		18	118	441	18224	14.2	3.2E-9	6.3	1.7E-7
KEGG_PATHWAY	Oxidative phosphorylation	RT		11	42	133	6879	8.7	3.5E-9	13.5	2.6E-7
GOTERM_CC_DIRECT	mitochondrial intermembrane space protein transporter complex	RT		5	118	5	18224	3.9	8.0E-9	154.4	3.2E-7
GOTERM_BP_DIRECT	chaperone-mediated protein transport	RT		5	110	8	16792	3.9	1.2E-7	95.4	6.0E-5
UP_KEYWORDS	Chaperone	RT		11	126	201	20581	8.7	4.2E-7	8.9	1.8E-5
KEGG_PATHWAY	Huntington's disease	RT		10	42	192	6879	7.9	1.4E-6	8.5	5.2E-5
GOTERM_BP_DIRECT	protein targeting to mitochondrion	RT		6	110	34	16792	4.7	2.5E-6	26.9	6.5E-4
GOTERM_CC_DIRECT	mediator complex	RT		6	118	35	18224	4.7	2.8E-6	26.5	8.9E-5
UP_KEYWORDS	Translocation	RT		7	126	84	20581	5.5	1.2E-5	13.6	4.2E-4
KEGG_PATHWAY	Parkinson's disease	RT		8	42	142	6879	6.3	1.7E-5	9.2	4.3E-4
UP_KEYWORDS	Transit peptide	RT		14	126	536	20581	11.0	2.3E-5	4.3	6.8E-4
UP_KEYWORDS	Transport	RT		28	126	1978	20581	22.0	4.6E-5	2.3	1.1E-3
KEGG_PATHWAY	Alzheimer's disease	RT		8	42	168	6879	6.3	5.1E-5	7.8	9.6E-4

Figure S8 – TMT iii.

Functional annotation clustering: **Functional annotation terms:**

SP4-GB / cSP3 80% ACN proteins (n=213):

Annotation Cluster 1	Enrichment Score: 6.48			Count	P_Value	Benjamini
KEGG_PATHWAY	Oxidative phosphorylation	RT		16	7.2E-11	1.1E-8
UP_KEYWORDS	Mitochondrion inner membrane	RT		19	4.3E-10	1.1E-7
KEGG_PATHWAY	Parkinson's disease	RT		15	2.0E-9	1.5E-7
UP_KEYWORDS	Mitochondrion	RT		33	1.5E-7	1.3E-5
GOTERM_CC_DIRECT	mitochondrial respiratory chain complex I	RT		8	1.0E-6	2.3E-4
UP_KEYWORDS	Ubiquinone	RT		7	1.4E-6	8.8E-5
UP_KEYWORDS	Electron transport	RT		10	1.8E-6	9.0E-5
GOTERM_CC_DIRECT	mitochondrial inner membrane	RT		19	1.9E-6	2.3E-4
UP_KEYWORDS	Respiratory chain	RT		8	3.8E-6	1.6E-4
GOTERM_MF_DIRECT	NADH dehydrogenase (ubiquinone) activity	RT		7	1.3E-5	4.1E-3
GOTERM_BP_DIRECT	mitochondrial electron transport, NADH to ubiquinone	RT		7	1.4E-5	1.3E-2
GOTERM_BP_DIRECT	mitochondrial respiratory chain complex I assembly	RT		7	5.9E-5	2.7E-2
Annotation Cluster 2	**Enrichment Score: 4.04**			**Count**	**P_Value**	**Benjamini**
KEGG_PATHWAY	Huntington's disease	RT		12	2.6E-5	1.0E-3
KEGG_PATHWAY	Non-alcoholic fatty liver disease (NAFLD)	RT		10	1.1E-4	3.4E-3
KEGG_PATHWAY	Alzheimer's disease	RT		10	2.5E-4	6.4E-3
Annotation Cluster 3	**Enrichment Score: 2.31**			**Count**	**P_Value**	**Benjamini**
GOTERM_CC_DIRECT	oligosaccharyltransferase complex	RT		4	1.5E-4	9.2E-3
KEGG_PATHWAY	N-Glycan biosynthesis	RT		5	3.3E-3	7.2E-2

Sublist	Category	Term	RT	Genes	Count	LT	PH	PT	%	P-Value	Fold Enrichment	Benjamini
	KEGG_PATHWAY	Oxidative phosphorylation	RT		16	80	133	6879	7.5	7.2E-11	9.4	1.1E-8
	UP_KEYWORDS	Mitochondrion inner membrane	RT		19	213	270	20581	8.9	4.3E-10	6.8	1.1E-7
	KEGG_PATHWAY	Parkinson's disease	RT		15	88	142	6879	7.0	2.0E-9	8.3	1.5E-7
	UP_KEYWORDS	Leber hereditary optic neuropathy	RT		6	213	10	20581	2.8	2.7E-8	58.0	3.4E-6
	UP_KEYWORDS	Mitochondrion	RT		33	213	1119	20581	15.5	1.5E-7	2.8	1.3E-5
	KEGG_PATHWAY	Metabolic pathways	RT		36	88	1219	6879	16.9	5.9E-7	2.3	3.0E-5
	GOTERM_CC_DIRECT	mitochondrial respiratory chain complex I	RT		8	201	49	18224	3.8	1.0E-6	14.8	2.3E-4
	UP_KEYWORDS	Ubiquinone	RT		7	213	35	20581	3.3	1.4E-6	19.3	8.8E-5
	UP_KEYWORDS	Electron transport	RT		10	213	108	20581	4.7	1.8E-6	8.9	9.0E-5
	GOTERM_CC_DIRECT	mitochondrial inner membrane	RT		19	201	441	18224	8.9	1.9E-6	3.9	2.3E-4
	UP_KEYWORDS	Respiratory chain	RT		8	213	63	20581	3.8	3.8E-6	12.3	1.6E-4
	UP_KEYWORDS	Transport	RT		43	213	1978	20581	20.2	4.5E-6	2.1	1.6E-4
	GOTERM_MF_DIRECT	NADH dehydrogenase (ubiquinone) activity	RT		7	186	48	16881	3.3	1.3E-5	13.2	4.1E-3
	GOTERM_BP_DIRECT	mitochondrial electron transport, NADH to ubiquinone	RT		7	182	49	16792	3.3	1.4E-5	13.2	1.3E-2
	KEGG_PATHWAY	Huntington's disease	RT		12	88	192	6879	5.6	2.6E-5	4.9	1.0E-3
	GOTERM_CC_DIRECT	endoplasmic reticulum membrane	RT		25	201	862	18224	11.7	2.7E-5	2.6	2.2E-3
	UP_KEYWORDS	Endoplasmic reticulum	RT		27	213	1067	20581	12.7	4.2E-5	2.4	1.3E-3
	GOTERM_BP_DIRECT	mitochondrial respiratory chain complex I assembly	RT		7	182	63	16792	3.3	5.9E-5	10.3	2.7E-2
	KEGG_PATHWAY	Non-alcoholic fatty liver disease (NAFLD)	RT		10	88	151	6879	4.7	1.1E-4	5.2	3.4E-3
	GOTERM_CC_DIRECT	oligosaccharyltransferase complex	RT		4	201	10	18224	1.9	1.5E-4	36.3	9.2E-3
	GOTERM_MF_DIRECT	protein binding	RT		122	186	8785	16881	57.3	1.5E-4	1.3	2.3E-2
	KEGG_PATHWAY	Alzheimer's disease	RT		10	88	168	6879	4.7	2.5E-4	4.7	6.4E-3
	GOTERM_CC_DIRECT	mitochondrion	RT		30	201	1331	18224	14.1	3.0E-4	2.0	1.5E-2

SP4-GB / cSP3 50% ACN proteins (n=246):

Annotation Cluster 1	Enrichment Score: 11.83			Count	P_Value	Benjamini
KEGG_PATHWAY	Oxidative phosphorylation	RT		23	1.6E-17	2.2E-15
KEGG_PATHWAY	Huntington's disease	RT		25	3.7E-16	2.4E-14
KEGG_PATHWAY	Parkinson's disease	RT		21	1.5E-14	6.6E-13
UP_KEYWORDS	Mitochondrion inner membrane	RT		23	1.3E-12	1.7E-10
GOTERM_CC_DIRECT	mitochondrial inner membrane	RT		28	9.2E-12	2.7E-9
KEGG_PATHWAY	Alzheimer's disease	RT		18	3.8E-10	1.2E-8
UP_KEYWORDS	Mitochondrion	RT		40	1.2E-9	1.0E-7
KEGG_PATHWAY	Non-alcoholic fatty liver disease (NAFLD)	RT		15	4.8E-8	1.3E-6
Annotation Cluster 2	**Enrichment Score: 6**			**Count**	**P_Value**	**Benjamini**
GOTERM_MF_DIRECT	cytochrome-c oxidase activity	RT		8	7.3E-8	2.4E-5
GOTERM_BP_DIRECT	mitochondrial electron transport, cytochrome c to oxygen	RT		7	1.2E-7	1.2E-4
GOTERM_BP_DIRECT	hydrogen ion transmembrane transport	RT		9	9.1E-7	4.5E-4
KEGG_PATHWAY	Cardiac muscle contraction	RT		8	1.3E-4	2.4E-3
Annotation Cluster 3	**Enrichment Score: 5.09**			**Count**	**P_Value**	**Benjamini**
INTERPRO	Tim10/DDP family zinc finger	RT		6	1.4E-9	5.7E-7
UP_SEQ_FEATURE	short sequence motif:Twin CX3C motif	RT		6	1.4E-9	9.6E-7
GOTERM_CC_DIRECT	mitochondrial intermembrane space protein transporter complex	RT		5	1.2E-7	1.1E-5
GOTERM_BP_DIRECT	chaperone-mediated protein transport	RT		5	1.6E-6	5.4E-4
UP_KEYWORDS	Translocation	RT		7	4.8E-4	1.3E-2

Sublist	Category	Term	RT	Genes	Count	LT	PH	PT	%	P-Value	Fold Enrichment	Benjamini
	KEGG_PATHWAY	Oxidative phosphorylation	RT		23	105	133	6879	9.3	1.6E-17	11.3	2.2E-15
	UP_KEYWORDS	Acetylation	RT		96	244	3424	20581	39.0	2.6E-17	2.4	7.0E-15
	KEGG_PATHWAY	Huntington's disease	RT		25	105	192	6879	10.2	3.7E-16	8.5	2.4E-14
	KEGG_PATHWAY	Parkinson's disease	RT		21	105	142	6879	8.5	1.5E-14	9.7	6.6E-13
	UP_KEYWORDS	Mitochondrion inner membrane	RT		23	244	270	20581	9.3	1.3E-12	7.2	1.7E-10
	GOTERM_CC_DIRECT	mitochondrial inner membrane	RT		28	228	441	18224	11.4	9.2E-12	5.1	2.7E-9
	KEGG_PATHWAY	Alzheimer's disease	RT		18	105	168	6879	7.3	3.8E-10	7.0	1.2E-8
	UP_KEYWORDS	Mitochondrion	RT		40	244	1119	20581	16.3	1.2E-9	3.0	1.0E-7
	INTERPRO	Tim10/DDP family zinc finger	RT		6	222	6	18559	2.4	1.4E-9	83.6	5.7E-7
	UP_SEQ_FEATURE	short sequence motif:Twin CX3C motif	RT		6	241	6	20063	2.4	1.4E-9	83.2	9.6E-7
	UP_KEYWORDS	Chaperone	RT		16	244	201	20581	6.5	1.0E-8	6.7	1.2E-6
	GOTERM_CC_DIRECT	mitochondrial intermembrane space	RT		11	228	74	18224	4.5	2.6E-8	11.9	3.9E-6
	KEGG_PATHWAY	Non-alcoholic fatty liver disease (NAFLD)	RT		15	105	151	6879	6.1	4.8E-8	6.5	1.3E-6
	GOTERM_MF_DIRECT	cytochrome-c oxidase activity	RT		8	214	30	16881	3.3	7.3E-8	21.0	2.4E-5
	GOTERM_CC_DIRECT	mitochondrial intermembrane space protein transporter complex	RT		5	228	5	18224	2.0	1.2E-7	79.9	1.1E-5
	GOTERM_BP_DIRECT	mitochondrial electron transport, cytochrome c to oxygen	RT		7	212	20	16792	2.8	1.2E-7	27.7	1.2E-4
	GOTERM_CC_DIRECT	mitochondrion	RT		40	228	1331	18224	16.3	4.6E-7	2.4	3.4E-5
	UP_KEYWORDS	Electron transport	RT		11	244	108	20581	4.5	6.2E-7	8.6	3.3E-5
	GOTERM_BP_DIRECT	hydrogen ion transmembrane transport	RT		9	212	61	16792	3.7	9.1E-7	11.7	4.5E-4
	KEGG_PATHWAY	Metabolic pathways	RT		40	105	1219	6879	16.3	1.2E-6	2.1	2.5E-5
	GOTERM_BP_DIRECT	chaperone-mediated protein transport	RT		5	212	8	16792	2.0	1.6E-6	49.5	5.4E-4
	GOTERM_CC_DIRECT	mitochondrial respiratory chain complex I	RT		8	228	49	18224	3.3	2.3E-6	13.0	1.4E-4
	UP_KEYWORDS	Respiratory chain	RT		8	244	63	20581	3.3	9.2E-6	10.7	4.1E-4

cSP3 (80+50 % ACN) / SP4-GB proteins (n=147, combined):

Annotation Cluster 1	Enrichment Score: 3.26			Count	P_Value	Benjamini
INTERPRO	Intermediate filament protein, conserved site	RT		6	1.1E-4	3.3E-2
UP_SEQ_FEATURE	region of interest:Coil 2	RT		6	1.2E-4	2.4E-2
UP_SEQ_FEATURE	region of interest:Linker 12	RT		6	1.2E-4	2.4E-2
SMART	SM01391	RT		6	1.3E-4	9.0E-3
UP_SEQ_FEATURE	region of interest:Coil 1A	RT		6	1.8E-4	2.4E-2
UP_SEQ_FEATURE	region of interest:Coil 1B	RT		6	1.8E-4	2.4E-2
UP_SEQ_FEATURE	region of interest:Linker 1	RT		6	1.8E-4	2.4E-2
UP_SEQ_FEATURE	region of interest:Rod	RT		6	1.9E-4	2.4E-2
UP_KEYWORDS	Intermediate filament	RT		6	2.1E-4	1.2E-2
UP_SEQ_FEATURE	region of interest:Head	RT		6	2.2E-4	2.4E-2
UP_SEQ_FEATURE	region of interest:Tail	RT		6	2.4E-4	2.4E-2
INTERPRO	Intermediate filament protein	RT		6	2.8E-4	4.2E-2

Sublist	Category	Term	RT	Genes	Count	LT	PH	PT	%	P-Value	Fold Enrichment	Benjamini
	UP_KEYWORDS	Acetylation	RT		46	145	3424	20581	31.3	1.1E-5	1.9	2.5E-3
	UP_KEYWORDS	Methylation	RT		21	145	1001	20581	14.3	2.2E-5	3.0	2.6E-3
	UP_KEYWORDS	Phosphoprotein	RT		82	145	8246	20581	55.8	6.0E-5	1.4	4.7E-3
	INTERPRO	Intermediate filament protein, conserved site	RT		6	138	64	18559	4.1	1.1E-4	12.6	3.3E-2
	UP_SEQ_FEATURE	region of interest:Coil 2	RT		6	143	68	20063	4.1	1.2E-4	12.4	2.4E-2
	UP_SEQ_FEATURE	region of interest:Linker 12	RT		6	143	68	20063	4.1	1.2E-4	12.4	2.4E-2
	SMART	SM01391	RT		6	67	75	10057	4.1	1.3E-4	12.0	9.0E-3
	UP_SEQ_FEATURE	region of interest:Coil 1A	RT		6	143	74	20063	4.1	1.8E-4	11.4	2.4E-2
	UP_SEQ_FEATURE	region of interest:Linker 1	RT		6	143	74	20063	4.1	1.8E-4	11.4	2.4E-2
	UP_SEQ_FEATURE	region of interest:Coil 1B	RT		6	143	74	20063	4.1	1.8E-4	11.4	2.4E-2
	UP_SEQ_FEATURE	region of interest:Rod	RT		6	143	75	20063	4.1	1.9E-4	11.2	2.4E-2
	UP_KEYWORDS	Intermediate filament	RT		6	145	77	20581	4.1	2.1E-4	11.1	1.2E-2
	GOTERM_MF_DIRECT	structural constituent of cytoskeleton	RT		7	131	110	16881	4.8	2.1E-4	8.2	4.9E-2
	UP_SEQ_FEATURE	region of interest:Head	RT		6	143	77	20063	4.1	2.2E-4	10.9	2.4E-2
	UP_SEQ_FEATURE	region of interest:Tail	RT		6	143	79	20063	4.1	2.4E-4	10.7	2.4E-2
	INTERPRO	Intermediate filament protein	RT		6	138	78	18559	4.1	2.8E-4	10.3	4.2E-2
	UP_KEYWORDS	Cytoplasm	RT		53	145	4816	20581	36.1	3.9E-4	1.6	1.8E-2

cSP3 80% ACN / cSP3 50% ACN proteins (n=220)

Annotation Cluster 1	Enrichment Score: 7.78			Count	P_Value	Benjamini
KEGG_PATHWAY	Huntington's disease	RT		18	8.4E-12	1.0E-9
KEGG_PATHWAY	Oxidative phosphorylation	RT		15	7.2E-11	4.4E-9
KEGG_PATHWAY	Alzheimer's disease	RT		15	1.7E-9	6.5E-8
KEGG_PATHWAY	Parkinson's disease	RT		14	2.1E-9	6.5E-8
GOTERM_CC_DIRECT	mitochondrial inner membrane	RT		22	1.4E-8	3.9E-6
KEGG_PATHWAY	Non-alcoholic fatty liver disease (NAFLD)	RT		12	4.4E-7	1.1E-5
KEGG_PATHWAY	Metabolic pathways	RT		21	2.6E-2	3.5E-1
Annotation Cluster 2	**Enrichment Score: 4.81**			**Count**	**P_Value**	**Benjamini**
INTERPRO	Tim10/DDP family zinc finger	RT		6	7.2E-10	2.5E-7
UP_SEQ_FEATURE	short sequence motif:Twin CX3C motif	RT		6	7.7E-10	7.3E-7
GOTERM_BP_DIRECT	chaperone-mediated protein transport	RT		6	7.9E-9	6.6E-6
GOTERM_CC_DIRECT	mitochondrial intermembrane space protein transporter complex	RT		5	6.6E-8	9.1E-6
UP_KEYWORDS	Translocation	RT		8	2.9E-5	1.4E-3
GOTERM_BP_DIRECT	protein targeting to mitochondrion	RT		6	3.1E-5	1.2E-2

Sublist	Category	Term	RT	Genes	Count	LT	PH	PT	%	P-Value	Fold Enrichment	Benjamini
	UP_KEYWORDS	Acetylation	RT		87	217	3424	20581	39.5	3.4E-16	2.4	7.9E-14
	KEGG_PATHWAY	Huntington's disease	RT		18	74	192	6879	8.2	8.4E-12	8.7	1.0E-9
	KEGG_PATHWAY	Oxidative phosphorylation	RT		15	74	133	6879	6.8	7.2E-11	10.5	4.4E-9
	INTERPRO	Tim10/DDP family zinc finger	RT		6	196	6	18559	2.7	7.2E-10	94.7	2.5E-7
	UP_SEQ_FEATURE	short sequence motif:Twin CX3C motif	RT		6	214	6	20063	2.7	7.7E-10	93.8	7.3E-7
	KEGG_PATHWAY	Alzheimer's disease	RT		15	74	168	6879	6.8	1.7E-9	8.3	6.5E-8
	KEGG_PATHWAY	Parkinson's disease	RT		14	74	142	6879	6.4	2.1E-9	9.2	6.5E-8
	GOTERM_BP_DIRECT	chaperone-mediated protein transport	RT		6	184	6	16792	2.7	7.9E-9	68.4	6.6E-6
	GOTERM_CC_DIRECT	mitochondrial inner membrane	RT		22	198	441	18224	10.0	1.4E-8	4.6	3.9E-6
	UP_KEYWORDS	Mitochondrion	RT		35	217	1119	20581	15.9	2.2E-8	3.0	2.6E-6
	GOTERM_CC_DIRECT	mitochondrial intermembrane space protein transporter complex	RT		5	198	5	18224	2.3	6.6E-8	92.0	9.1E-6
	GOTERM_CC_DIRECT	mitochondrial intermembrane space	RT		10	198	74	18224	4.5	1.0E-7	12.4	9.3E-6
	UP_KEYWORDS	Mitochondrion inner membrane	RT		16	217	270	20581	7.3	1.8E-7	5.6	1.3E-5
	UP_KEYWORDS	Chaperone	RT		14	217	201	20581	6.4	2.2E-7	6.6	1.3E-5
	KEGG_PATHWAY	Non-alcoholic fatty liver disease (NAFLD)	RT		12	74	151	6879	5.5	4.4E-7	7.4	1.1E-5
	GOTERM_CC_DIRECT	mitochondrion	RT		35	198	1331	18224	15.9	2.2E-6	2.4	1.5E-4
	INTERPRO	Ubiquitin	RT		8	196	59	18559	3.6	2.7E-6	12.8	4.7E-4
	GOTERM_MF_DIRECT	protein binding	RT		127	185	8785	16881	57.7	3.9E-6	1.3	1.0E-3
	INTERPRO	Prefoldin	RT		6	196	26	18559	2.7	6.7E-6	21.9	7.6E-4
	SMART	UBQ	RT		6	71	43	10057	2.7	1.1E-5	19.8	4.5E-4
	SMART	SM01391	RT		7	71	75	10057	3.2	1.3E-5	13.2	4.5E-4
	GOTERM_MF_DIRECT	cytochrome-c oxidase activity	RT		6	185	30	16881	2.7	1.7E-5	18.2	2.1E-3
	UP_SEQ_FEATURE	region of interest:Head	RT		8	214	77	20063	3.6	1.8E-5	9.7	6.6E-3
	UP_SEQ_FEATURE	region of interest:Tail	RT		8	214	79	20063	3.6	2.1E-5	9.5	6.6E-3
	INTERPRO	Ubiquitin	RT		4	196	6	18559	1.8	2.2E-5	63.1	1.9E-3
	UP_KEYWORDS	Translocation	RT		8	217	84	20581	3.6	2.9E-5	9.0	1.4E-3
	GOTERM_BP_DIRECT	protein targeting to mitochondrion	RT		6	184	34	16792	2.7	3.1E-5	16.1	1.2E-2
	GOTERM_CC_DIRECT	prefoldin complex	RT		4	198	7	18224	1.8	4.2E-5	52.6	2.3E-3
	GOTERM_BP_DIRECT	hydrogen ion transmembrane transport	RT		7	184	61	16792	3.2	5.2E-5	10.5	1.2E-2
	INTERPRO	Intermediate filament protein, conserved site	RT		7	196	64	18559	3.2	5.6E-5	10.4	3.8E-3
	GOTERM_BP_DIRECT	mitochondrial electron transport, cytochrome c to oxygen	RT		5	184	20	16792	2.3	5.8E-5	22.8	1.2E-2

Figure S8 – TMT iv.

Functional annotation clustering: **Functional annotation terms:**

SP4-GB / S-Trap proteins (n=265):

Annotation Cluster 1	Enrichment Score: 6.55		Count	P_Value	Fold Change	Benjamini
UP_KEYWORDS	Ribonucleoprotein	RT	21	1.4E-9	5.6E0	2.0E-7
GOTERM_CC_DIRECT	cytosolic large ribosomal subunit	RT	12	1.6E-9	1.3E1	5.0E-7
GOTERM_MF_DIRECT	structural constituent of ribosome	RT	18	1.1E-8	5.9E0	4.0E-6
KEGG_PATHWAY	Ribosome	RT	16	1.4E-8	6.5E0	2.2E-6
UP_KEYWORDS	Ribosomal protein	RT	16	1.5E-8	6.8E0	1.5E-6
GOTERM_BP_DIRECT	SRP-dependent cotranslational protein targeting to membrane	RT	12	7.9E-8	9.1E0	4.0E-5
GOTERM_BP_DIRECT	translation	RT	18	1.0E-7	5.1E0	4.0E-5
GOTERM_BP_DIRECT	nuclear-transcribed mRNA catabolic process, nonsense-mediated decay	RT	13	1.1E-7	7.8E0	4.0E-5
GOTERM_BP_DIRECT	viral transcription	RT	12	4.8E-7	7.6E0	1.1E-4
GOTERM_BP_DIRECT	translational initiation	RT	13	5.1E-7	6.8E0	1.1E-4
GOTERM_CC_DIRECT	ribosome	RT	13	2.6E-6	5.8E0	3.5E-4
GOTERM_BP_DIRECT	rRNA processing	RT	14	1.0E-5	4.7E0	1.9E-3
GOTERM_BP_DIRECT	cytoplasmic translation	RT	5	3.8E-4	1.4E1	5.3E-2
GOTERM_MF_DIRECT	poly(A) RNA binding	RT	29	1.7E-3	1.9E0	2.0E-1
Annotation Cluster 2	**Enrichment Score: 5.17**		**Count**	**P_Value**	**Fold Change**	**Benjamini**
UP_KEYWORDS	Mitochondrion inner membrane	RT	17	3.9E-7	4.9E0	2.8E-5
UP_KEYWORDS	Mitochondrion	RT	34	5.8E-6	2.4E0	3.2E-4
GOTERM_CC_DIRECT	mitochondrial inner membrane	RT	20	8.7E-6	3.4E0	6.7E-4
GOTERM_CC_DIRECT	mitochondrion	RT	36	1.0E-4	2.0E0	6.3E-3

Category	Term	RT	Genes	Count	LT	PH	PT	%	P-Value	Fold Enrichment	Benjamini
UP_KEYWORDS	Acetylation	RT		95	262	3424	20581	35.8	2.3E-14	2.2	6.6E-12
UP_KEYWORDS	Ribonucleoprotein	RT		21	262	296	20581	7.9	1.4E-9	5.6	2.0E-7
GOTERM_CC_DIRECT	cytosolic large ribosomal subunit	RT		12	246	68	18224	4.5	1.6E-9	13.1	5.0E-7
GOTERM_MF_DIRECT	structural constituent of ribosome	RT		18	232	222	16881	6.8	1.1E-8	5.9	4.0E-6
KEGG_PATHWAY	Ribosome	RT		16	124	136	6879	6.0	1.4E-8	6.5	2.2E-6
UP_KEYWORDS	Ribosomal protein	RT		16	262	185	20581	6.0	1.5E-8	6.8	1.5E-6
GOTERM_BP_DIRECT	SRP-dependent cotranslational protein targeting to membrane	RT		12	236	94	16792	4.5	7.9E-8	9.1	4.0E-5
GOTERM_BP_DIRECT	translation	RT		18	236	253	16792	6.8	1.0E-7	5.1	4.0E-5
GOTERM_BP_DIRECT	nuclear-transcribed mRNA catabolic process, nonsense-mediated decay	RT		13	236	119	16792	4.9	1.1E-7	7.8	4.0E-5
UP_KEYWORDS	Mitochondrion inner membrane	RT		17	262	270	20581	6.4	3.9E-7	4.9	2.8E-5
GOTERM_BP_DIRECT	viral transcription	RT		12	236	112	16792	4.5	4.8E-7	7.6	1.1E-4
GOTERM_BP_DIRECT	translational initiation	RT		13	236	137	16792	4.9	5.1E-7	6.8	1.1E-4
GOTERM_CC_DIRECT	ribosome	RT		13	246	166	18224	4.9	2.6E-6	5.8	3.5E-4
GOTERM_CC_DIRECT	nucleoplasm	RT		66	246	2784	18224	24.9	3.4E-6	1.8	3.5E-4
UP_KEYWORDS	Mitochondrion	RT		34	262	1119	20581	12.8	5.8E-6	2.4	3.3E-4
GOTERM_CC_DIRECT	mitochondrial inner membrane	RT		20	246	441	18224	7.5	8.7E-6	3.4	6.7E-4
GOTERM_BP_DIRECT	rRNA processing	RT		14	236	214	16792	5.3	1.0E-5	4.7	1.9E-3
GOTERM_MF_DIRECT	protein binding	RT		152	232	8785	16881	57.4	2.5E-5	1.3	4.5E-3
GOTERM_BP_DIRECT	mRNA splicing, via spliceosome	RT		13	236	222	16792	4.9	7.1E-5	4.2	1.1E-2
UP_KEYWORDS	Phosphoprotein	RT		136	262	8246	20581	51.3	8.3E-5	1.3	4.0E-3

S-Trap / SP4-GB proteins (n=185):

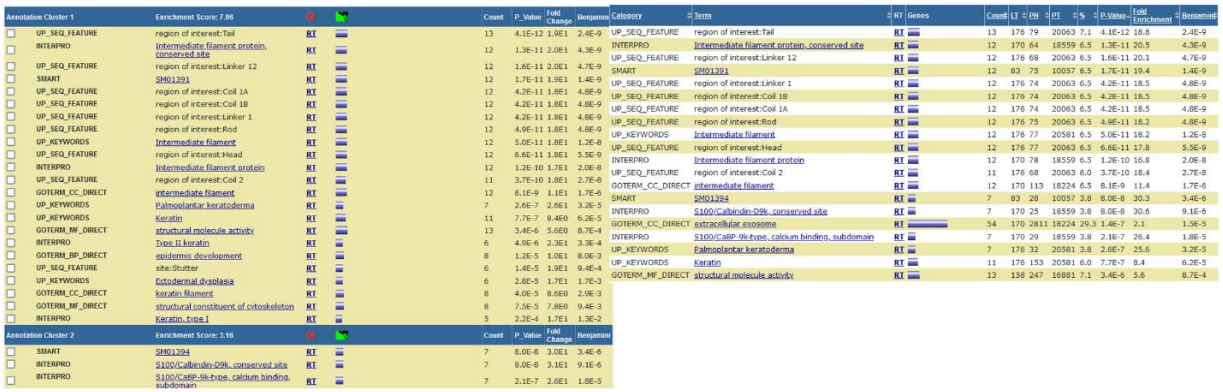

Annotation Cluster 1	Enrichment Score: 7.96		Count	P_Value	Fold Change	Benjamini
UP_SEQ_FEATURE	region of interest:Tail	RT	13	4.1E-12	1.9E1	2.4E-9
INTERPRO	Intermediate filament protein, conserved site	RT	12	1.3E-11	2.0E1	4.3E-9
UP_SEQ_FEATURE	region of interest:Linker 12	RT	12	1.6E-11	2.0E1	4.7E-9
SMART	SM01391	RT	12	1.7E-11	1.9E1	1.4E-9
UP_SEQ_FEATURE	region of interest:Coil 1A	RT	12	4.2E-11	1.8E1	4.8E-9
UP_SEQ_FEATURE	region of interest:Coil 1B	RT	12	4.2E-11	1.8E1	4.8E-9
UP_SEQ_FEATURE	region of interest:Linker 1	RT	12	4.2E-11	1.8E1	4.8E-9
UP_SEQ_FEATURE	region of interest:Rod	RT	12	4.9E-11	1.8E1	4.8E-9
UP_KEYWORDS	Intermediate filament	RT	12	5.0E-11	1.8E1	1.2E-8
UP_SEQ_FEATURE	region of interest:Head	RT	12	6.6E-11	1.8E1	5.5E-9
INTERPRO	Intermediate filament protein	RT	12	1.2E-10	1.7E1	2.0E-8
UP_SEQ_FEATURE	region of interest:Coil 2	RT	11	3.7E-10	1.8E1	2.7E-8
GOTERM_CC_DIRECT	intermediate filament	RT	12	8.1E-9	1.1E1	1.7E-6
UP_KEYWORDS	Palmoplantar keratoderma	RT	7	2.6E-7	2.6E1	3.2E-5
UP_KEYWORDS	Keratin	RT	11	7.7E-7	8.4E0	6.2E-5
GOTERM_MF_DIRECT	structural molecule activity	RT	13	3.4E-6	5.6E0	8.7E-4
INTERPRO	Type II keratin	RT	6	4.9E-6	2.3E1	3.3E-4
GOTERM_BP_DIRECT	epidermis development	RT	8	1.2E-5	1.0E1	8.0E-3
UP_SEQ_FEATURE	site:Stutter	RT	6	1.4E-5	1.9E1	9.4E-4
UP_KEYWORDS	Ectodermal dysplasia	RT	6	2.8E-5	1.7E1	1.7E-3
GOTERM_CC_DIRECT	keratin filament	RT	8	4.0E-5	8.6E0	2.9E-3
GOTERM_MF_DIRECT	structural constituent of cytoskeleton	RT	8	7.3E-5	7.8E0	9.4E-3
INTERPRO	Keratin, type I	RT	5	2.2E-4	1.7E1	1.3E-2
Annotation Cluster 2	**Enrichment Score: 3.16**		**Count**	**P_Value**	**Fold Change**	**Benjamini**
SMART	SM01394	RT	7	8.0E-8	3.0E1	3.4E-6
INTERPRO	S100/Calbindin-D9k, conserved site	RT	7	8.0E-8	3.1E1	9.1E-6
INTERPRO	S100/CaBP-9k-type, calcium binding, subdomain	RT	7	2.1E-7	2.6E1	1.8E-5

Category	Term	RT	Genes	Count	LT	PH	PT	%	P-Value	Fold Enrichment	Benjamini
UP_SEQ_FEATURE	region of interest:Tail	RT		13	176	79	20063	7.1	4.1E-12	16.8	2.4E-9
INTERPRO	Intermediate filament protein, conserved site	RT		12	170	64	18559	6.5	1.3E-11	20.5	4.3E-9
UP_SEQ_FEATURE	region of interest:Linker 12	RT		12	176	68	20063	6.5	1.6E-11	20.1	4.7E-9
SMART	SM01391	RT		12	83	75	10057	6.5	1.7E-11	19.4	1.4E-9
UP_SEQ_FEATURE	region of interest:Linker 1	RT		12	176	74	20063	6.5	4.2E-11	18.5	4.8E-9
UP_SEQ_FEATURE	region of interest:Coil 1B	RT		12	176	74	20063	6.5	4.2E-11	18.5	4.8E-9
UP_SEQ_FEATURE	region of interest:Coil 1A	RT		12	176	74	20063	6.5	4.2E-11	18.5	4.8E-9
UP_SEQ_FEATURE	region of interest:Rod	RT		12	176	75	20063	6.5	4.9E-11	18.2	4.8E-9
UP_KEYWORDS	Intermediate filament	RT		12	176	77	20581	6.5	5.0E-11	18.2	1.2E-8
UP_SEQ_FEATURE	region of interest:Head	RT		12	176	77	20063	6.5	6.6E-11	17.8	5.5E-9
INTERPRO	Intermediate filament protein	RT		12	170	78	18559	6.5	1.2E-10	16.8	2.0E-8
UP_SEQ_FEATURE	region of interest:Coil 2	RT		11	176	68	20063	6.0	3.7E-10	18.4	2.7E-8
GOTERM_CC_DIRECT	intermediate filament	RT		12	170	113	18224	6.5	8.1E-9	11.4	1.7E-6
SMART	SM01394	RT		7	83	28	10057	3.8	8.0E-8	30.3	3.4E-6
INTERPRO	S100/Calbindin-D9k, conserved site	RT		7	170	25	18559	3.8	8.0E-8	30.6	9.1E-6
GOTERM_CC_DIRECT	extracellular exosome	RT		54	170	2811	18224	29.3	1.4E-7	2.1	1.5E-5
INTERPRO	S100/CaBP-9k-type, calcium binding, subdomain	RT		7	170	29	18559	3.8	2.1E-7	26.4	1.8E-5
UP_KEYWORDS	Palmoplantar keratoderma	RT		7	176	32	20581	3.8	2.6E-7	25.6	3.2E-5
UP_KEYWORDS	Keratin	RT		11	176	153	20581	6.0	7.7E-7	8.4	6.2E-5
GOTERM_MF_DIRECT	structural molecule activity	RT		13	158	247	16881	7.1	3.4E-6	5.6	8.7E-4

SP4-GB / Spin filter proteins (n=102):

Annotation Cluster 1	Enrichment Score: 3.45		Count	P_Value	Fold Change	Benjamini
UP_KEYWORDS	Endoplasmic reticulum	RT	18	1.6E-5	3.4E0	1.1E-3
GOTERM_CC_DIRECT	endoplasmic reticulum membrane	RT	15	2.0E-4	3.2E0	3.7E-2
GOTERM_CC_DIRECT	endoplasmic reticulum	RT	11	1.4E-2	2.4E0	3.5E-1
Annotation Cluster 2	**Enrichment Score: 3.12**		**Count**	**P_Value**	**Fold Change**	**Benjamini**
UP_KEYWORDS	ER-Golgi transport	RT	7	6.9E-6	1.5E1	6.8E-4
UP_KEYWORDS	Golgi apparatus	RT	13	6.2E-4	3.2E0	2.4E-2
GOTERM_BP_DIRECT	ER to Golgi vesicle-mediated transport	RT	6	2.0E-3	6.7E0	3.5E-1
GOTERM_CC_DIRECT	Golgi membrane	RT	8	4.0E-2	2.5E0	4.8E-1
Annotation Cluster 3	**Enrichment Score: 2.94**		**Count**	**P_Value**	**Fold Change**	**Benjamini**
UP_SEQ_FEATURE	topological domain:Mitochondrial matrix	RT	4	3.3E-4	2.9E1	9.6E-2
UP_KEYWORDS	Mitochondrion inner membrane	RT	7	2.2E-3	5.2E0	6.0E-2
UP_SEQ_FEATURE	topological domain:Mitochondrial intermembrane	RT	4	2.2E-3	1.5E1	3.1E-1
Annotation Cluster 4	**Enrichment Score: 2.67**		**Count**	**P_Value**	**Fold Change**	**Benjamini**
GOTERM_BP_DIRECT	phosphatidylinositol dephosphorylation	RT	4	3.1E-4	3.0E1	8.3E-2
GOTERM_MF_DIRECT	inositol-1,4,5-trisphosphate 5-phosphatase activity	RT	3	4.2E-4	9.3E1	6.3E-2
SMART	IPPc	RT	3	4.6E-4	8.9E1	2.1E-2

Category	Term	RT	Genes	Count	LT	PH	PT	%	P-Value	Fold Enrichment	Benjamini
UP_KEYWORDS	Transport	RT		28	102	1978	20581	27.5	6.5E-7	2.9	1.3E-4
UP_KEYWORDS	ER-Golgi transport	RT		7	102	94	20581	6.9	6.9E-6	15.0	6.8E-4
UP_KEYWORDS	Endoplasmic reticulum	RT		18	102	1067	20581	17.6	1.6E-5	3.4	1.1E-3
UP_KEYWORDS	Protein transport	RT		13	102	610	20581	12.7	4.4E-5	4.3	2.2E-3
GOTERM_BP_DIRECT	protein transport	RT		11	94	395	16792	10.8	6.6E-5	5.0	3.6E-2
GOTERM_CC_DIRECT	endoplasmic reticulum membrane	RT		15	99	862	18224	14.7	2.0E-4	3.2	3.7E-2
GOTERM_BP_DIRECT	phosphatidylinositol dephosphorylation	RT		4	94	24	16792	3.9	3.1E-4	29.8	8.3E-2
UP_SEQ_FEATURE	topological domain:Mitochondrial matrix	RT		4	102	27	20063	3.9	3.3E-4	29.1	9.6E-2
GOTERM_MF_DIRECT	inositol-1,4,5-trisphosphate 5-phosphatase activity	RT		3	91	6	16881	2.9	4.2E-4	92.8	6.3E-2
SMART	IPPc	RT		3	34	10	10057	2.9	4.6E-4	88.7	2.1E-2
GOTERM_CC_DIRECT	membrane	RT		25	99	2200	18224	24.5	4.9E-4	2.1	4.1E-2
UP_KEYWORDS	Golgi apparatus	RT		13	102	812	20581	12.7	6.2E-4	3.2	2.4E-2
GOTERM_CC_DIRECT	mitochondrion	RT		18	99	1331	18224	17.6	6.9E-4	2.5	4.1E-2

S-Trap / Spin filter proteins (n=102):

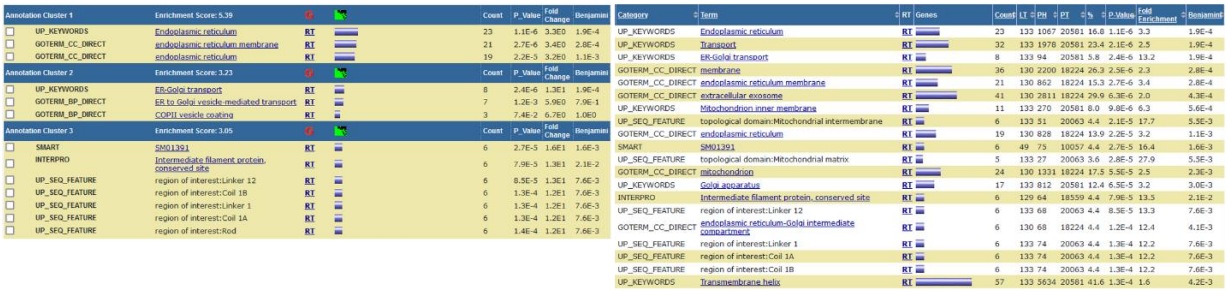

Annotation Cluster 1	Enrichment Score: 5.39		Count	P_Value	Fold Change	Benjamini
UP_KEYWORDS	Endoplasmic reticulum	RT	23	1.1E-6	3.2E0	1.9E-4
GOTERM_CC_DIRECT	endoplasmic reticulum membrane	RT	21	2.7E-6	3.4E0	2.0E-4
GOTERM_CC_DIRECT	endoplasmic reticulum	RT	19	2.2E-3	3.2E0	1.1E-3
Annotation Cluster 2	**Enrichment Score: 3.23**		**Count**	**P_Value**	**Fold Change**	**Benjamini**
UP_KEYWORDS	ER-Golgi transport	RT	8	2.4E-6	1.3E1	1.9E-4
GOTERM_BP_DIRECT	ER to Golgi vesicle-mediated transport	RT	7	1.2E-3	5.9E0	7.9E-1
GOTERM_BP_DIRECT	COPII vesicle coating	RT	3	7.4E-2	6.7E0	1.0E0
Annotation Cluster 3	**Enrichment Score: 3.05**		**Count**	**P_Value**	**Fold Change**	**Benjamini**
SMART	SM01391	RT	6	2.7E-5	1.6E1	1.6E-3
INTERPRO	Intermediate filament protein, conserved site	RT	6	7.9E-5	1.3E1	2.1E-2
UP_SEQ_FEATURE	region of interest:Linker 12	RT	6	8.5E-5	1.3E1	7.6E-3
UP_SEQ_FEATURE	region of interest:Coil 1B	RT	6	1.3E-4	1.2E1	7.6E-3
UP_SEQ_FEATURE	region of interest:Linker 1	RT	6	1.3E-4	1.2E1	7.6E-3
UP_SEQ_FEATURE	region of interest:Coil 1A	RT	6	1.3E-4	1.2E1	7.6E-3
UP_SEQ_FEATURE	region of interest:Rod	RT	6	1.4E-4	1.2E1	7.6E-3

Category	Term	RT	Genes	Count	LT	PH	PT	%	P-Value	Fold Enrichment	Benjamini
UP_KEYWORDS	Endoplasmic reticulum	RT		23	133	1067	20581	16.8	1.1E-6	3.3	1.9E-4
UP_KEYWORDS	Transport	RT		32	133	1978	20581	23.4	2.1E-6	2.5	1.9E-4
UP_KEYWORDS	ER-Golgi transport	RT		8	133	94	20581	5.8	2.4E-6	13.2	1.9E-4
GOTERM_CC_DIRECT	membrane	RT		36	130	2200	18224	26.3	2.5E-6	2.3	2.8E-4
GOTERM_CC_DIRECT	endoplasmic reticulum membrane	RT		21	130	862	18224	15.3	2.7E-6	3.4	2.8E-4
GOTERM_CC_DIRECT	extracellular exosome	RT		41	130	2811	18224	29.9	6.3E-6	2.0	4.3E-4
UP_KEYWORDS	Mitochondrion inner membrane	RT		11	133	270	20581	8.0	9.8E-6	6.3	5.6E-4
UP_SEQ_FEATURE	topological domain:Mitochondrial intermembrane	RT		6	133	51	20063	4.4	2.1E-5	17.7	5.3E-3
GOTERM_CC_DIRECT	endoplasmic reticulum	RT		19	130	828	18224	13.9	2.2E-5	3.2	1.1E-3
SMART	SM01391	RT		6	49	73	10057	4.4	2.7E-5	16.4	1.6E-3
UP_SEQ_FEATURE	topological domain:Mitochondrial matrix	RT		5	133	27	20063	3.6	2.8E-5	27.9	5.3E-3
GOTERM_CC_DIRECT	mitochondrion	RT		24	130	1331	18224	17.5	5.5E-5	2.5	2.3E-3
UP_KEYWORDS	Golgi apparatus	RT		17	133	812	20581	12.4	6.5E-5	3.2	3.0E-3
INTERPRO	Intermediate filament protein, conserved site	RT		6	129	64	18559	4.4	7.9E-5	13.5	2.1E-2
UP_SEQ_FEATURE	region of interest:Linker 12	RT		6	133	68	20063	4.4	8.5E-5	13.3	7.6E-3
GOTERM_CC_DIRECT	endoplasmic reticulum-Golgi intermediate compartment	RT		6	130	68	18224	4.4	1.2E-4	12.4	4.1E-3
UP_SEQ_FEATURE	region of interest:Linker 1	RT		6	133	74	20063	4.4	1.3E-4	12.2	7.6E-3
UP_SEQ_FEATURE	region of interest:Coil 1A	RT		6	133	74	20063	4.4	1.3E-4	12.2	7.6E-3
UP_SEQ_FEATURE	region of interest:Coil 1B	RT		6	133	74	20063	4.4	1.3E-4	12.2	7.6E-3
UP_KEYWORDS	Transmembrane helix	RT		57	133	5634	20581	41.6	1.3E-4	1.6	4.2E-3

Figure S8. **DAVID-derived term enrichment and clustering for those proteins observed more significantly recovered by SP3 and SP4 by TMT quantification (Fig 2D).** The human Swissprot UniProt proteome was used as a background. See also: Fig 2F, a summary of a more concise, GO-SLIM analysis of the cellular compartment terms for these protein subsets.

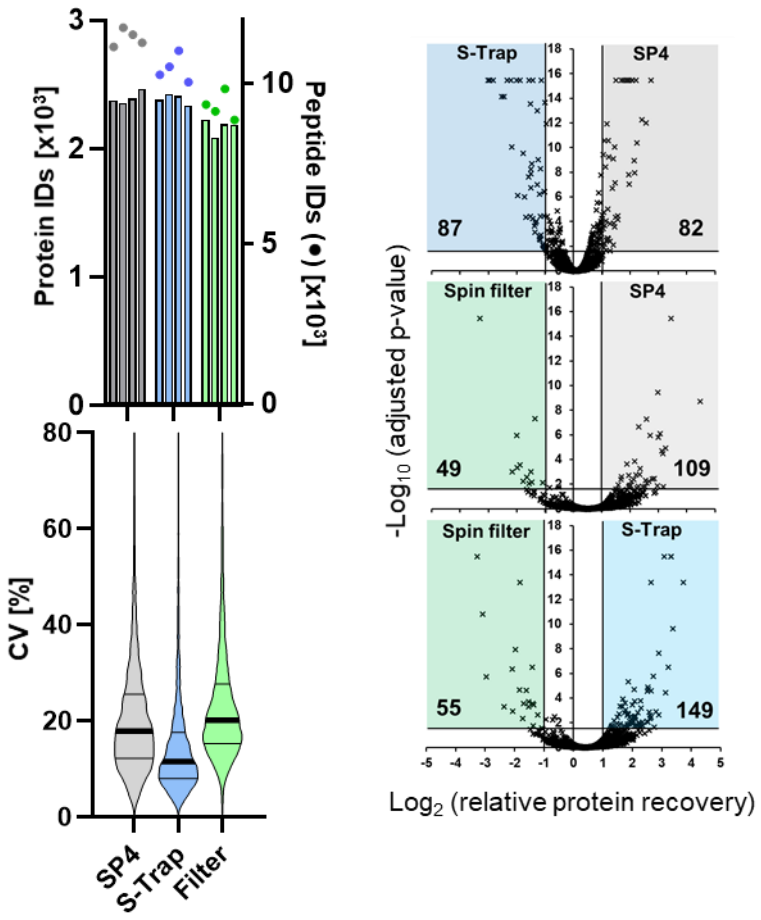

Figure S9. A label-free comparison of proteomics preparations by SP4, S-Trap, and precipitate capture by 0.22 *µ*m nylon spin filters. Protein (bars) and peptide (dots) identifications, protein coefficients of variance distributions (violin plot, thick bar – median, thin bars - quartiles) and volcano plots describing significant differential recovery for 100 *µ*g of HEK293 lysate prepared by SP4, S-Trap, and precipitate capture by 0.22 *µ*m nylon spin filters. See also: Fig 2-iv, a higher-depth proteome characterisation by TMT.

Supplementary Methods

Materials. Dulbecco's Modified Eagle Medium (DMEM), 100x pen-strep, 100x L-glutamine, 100x MEM non-essential amino acids (NEAA), and UltraPure Tris were purchased from Invitrogen; HyClone foetal bovine serum (FBS) from Fisher Scientific; cOmplete mini EDTA-free protease inhibitors from Roche; BCA and peptide quantitation assays, TMT 6-plex, and LC-MS grade ACN from Thermo Scientific; HEPES from Melford Laboratories; NP-40 from Biovision; NaCl and urea from VWR International; glycerol, NaOH and LC-grade ACN from Fisher; SpeedBeads magnetic carboxylate modified particles 45152105050250 and 65152105050250 from Cytiva (GE Healthcare); Protein LoBind tubes from Eppendorf; Trypsin (V5111) and Lys-C from Promega, Costar Spin-X 0.22 μm nylon centrifugal filters from Corning; and S-Trap mini columns from Protifi. All other reagents were purchased from Sigma-Aldrich. Additional reagents used for validation are described for each lab.

Cell culture and lysis. HEK293 cells were grown in DMEM supplemented with 10% fetal bovine serum with 1x pen-strep, L-glutamine, and NEAA, in a humidified incubator set at 37 °C and 5% CO_2. Cells were grown to 70–80% confluency and were washed twice with phosphate buffered saline. Cells were harvested by scraping, pelleted at 300*g* for 5 min and snap-frozen in liquid nitrogen.

Detergent-based lysis was performed resuspending snap-frozen cell pellets in 'SP3 lysis buffer' (50 mM HEPES pH 8.0, 1% SDS, 1% Triton X-100, 1% NP-40, 1% Tween 20, 1% sodium deoxycholate, 50 mM NaCl, 10 mM DTT, 5 mM EDTA, 1% (w/v) glycerol, 1× cOmplete protease inhibitor tablet, 40 mM 2-chloroacetamide (CAA)). Lysis was conducted by trituration with a 23-gauge needle, incubated at 95 °C for 5 min, cooled to RT for 10 min, sonicated on ice for 12× 5 s bursts with 5 s intervals and cleared at 16,000*g* for 10 min at 4 °C. Protein concentration was estimated by BCA assay, Pierce 660nm Protein Assay, or NanoDrop 2000 (Thermo Scientific) at 280 nm.

Urea-based lysis was performed in-flask with urea buffer (8 M Urea, 50 mM Tris-HCl pH 8.0, 75 mM NaCl, 1 mM EDTA, 1× cOmplete protease inhibitor) and lysate snap-frozen in liquid nitrogen. Defrosted lysate was triturated 20× on ice and cleared at 16,000*g* for 10 min at 4 °C. Protein concentration was estimated by BCA assay according to manufacturer's instructions. Protein was reduced using 5 mM DTT for 45 min at 25 °C and alkylated with 10 mM CAA for 45 min at 25 °C.

'SPEED' lysis was performed as described previously (1). Briefly, an aliquoted cell pellet was lysed in 100% TFA, neutralised in 2 M Tris, and reduced and alkylated with 10 mM DTT and 40 mM CAA. The lysate was diluted 1:1 with water and precipitated according the SP4 protocol below with 10:1 glass bead:protein ratio.

Preparation of complex lysates. Whole tissue homogenates of mouse heart and lungs were prepared from 3× washed organs on ice using a gentleMACS tissue dissociator (Miltenyi Biotec) in PBS to single-cell suspensions using the recommended setting for each organ and centrifuged at 300*g* for 3 min at 4 °C. Pellets were lysed in SP3 lysis buffer and handled as described above, using additional sonication and no trituration. FFPE cross sections were incubated twice in xylene for 2 min, washed sequentially with 90, 70, 50, 70, 90, and 100% ethanol, incubated in xylene for 5 min and air dried. Tissue was solubilised in SP3 lysis buffer using a Bioruptor sonicator (Diagenode) for 22.5 min (15 cycles: 1 min on, 30 s off) at the highest setting at 4 °C. Lysates were incubated for 1 h at 99 °C. The samples were returned to the Bioruptor and the 1 h incubation was repeated. Lysates were cleared at 16,000*g* for 5 min and the supernatant was quantitated, reduced and alkylated, as above, for SP3 and SP4 processing. For whole *Drosophila melanogaster* homogenates, adult w^{1118} flies were transferred to a 1.5 mL microcentrifuge tube and immobilized by placing them at 4 °C for 5 min. The flies were then solubilised in ice-cold SP3 lysis buffer using a 1.5 mL tube-compatible pestle (Bel-Art, F65000-0006) and the lysate cleared twice at 16,000*g* for 10 min at 4 °C. Lysates were handled as above for SP3 and SP4.

Bead preparation. SpeedBeads magnetic carboxylate-modified particles (catalogue no. 45152105050250 and 65152105050250) were mixed 1:1, washed 3 times using Milli-Q® water, and resuspended at 50 mg/mL.

Silica beads/glass spheres (9–13 μm mean particle diameter, catalogue no. 440345) were suspended at an initial concentration of 100 mg/mL in Milli-Q water, washed with 100% ACN and 100 mM ammonium bicarbonate (ABC), and at least twice more with water. With each wash, the beads were pelleted by centrifugation at 16,000*g* for 1 min and the supernatant discarded. Of note: approximately 50% of the beads were buoyant and did not pellet, and were carefully removed over the course of these wash steps. Metal filings were noted to be a contaminant in the beads and can either be removed by magnet or acid wash, but did not impact any analyses. The beads were then resuspended in the initial suspension volume at 50 mg/mL (given ~50% were retained) in Milli-Q water. Alternatively, the beads were resuspended in 100% ACN at a concentration of at least 2.5× the protein concentration (detailed in the protocol) to allow simultaneous addition of beads and ACN, ensuring uniform bead suspension during aggregation and removing the need to add additional volumes.

SP3/SP4 protein aggregation/precipitation. Lysates were aliquoted into Protein LoBind tubes for each method and replicate. For SP4, 0.5 mL tubes were used (where volumes allowed) to give the densest pellet. Either 10:1 bead:protein ratio, or the equivalent volume of Milli-Q water (for the bead-free experiments, to maintain consistent concentrations), was added to lysates and gently vortex-mixed (< 500 rpm). Samples were handled such that liquid volume was minimised. 100% ACN was added (without pipette mixing) to a final concentration of 80% and tubes gently vortexed for 5 s. SP3 samples were incubated at 25 °C for 5 min at 800 rpm on a Thermomixer Comfort and placed on a magnetic rack for 2 min. SP4 samples were centrifuged for 5 min at 16,000*g*. Supernatants were removed carefully, using the tube hinge to orientate pellets. Three wash steps were performed with at least twice the total precipitation reaction volume of 80% ethanol, with buffer added slowly and avoiding disturbing the beads/pellet. Each wash used either a 2 min magnetic separation (SP3) or 2 min centrifugation at 16,000*g* (SP4).

For centrifugal SP3, the SP3 protocol was followed replacing magnetic isolation with 5 min and 2 min centrifugation steps at 16,000*g*.

Proteolysis and peptide isolation. After the final wash, remaining supernatant (bar < 5 μL) was carefully removed, the protein aggregates resuspended by gently vortexing the pellet in 100 mM ABC with 1:100 trypsin:protein ratio, and placed in a sonicator bath for 5 min. For the 500 and 5000 μg samples, 1:100 TrypZean (T3568, Sigma-Aldrich) was used in place of trypsin. Samples were incubated for 18 h at 37 °C at 1000 rpm on a Thermomixer Comfort. Peptide-containing supernatants were isolated by removal of magnetic beads (magrack, SP3) or beads and insoluble debris (16,000*g*, SP4) for 2 min.

Peptide quantitation assay. Peptide yields for optimization were determined using the Pierce Quantitative Fluorometric Peptide Assay (Thermo Scientific) according to manufacturer's instructions. For initial optimization, samples were prepared as above, varying acetonitrile concentration, bead:protein ratio, and centrifugation time while otherwise using 80% ACN, 5/2 min capture/wash centrifugation, and a 10:1 bead:protein ratio. Samples for each condition (n = 4) were digested in 50 μL of 20 mM ABC, and 10 μL were analysed in triplicate. For evaluation of SP3 and SP4 protein input concentrations on peptide recovery, 50 μg of HEK293 protein was aliquoted (n = 3), diluted from 5 to 0.63 μg/μL, and processed as described above.

S-Trap, spin filter, and SP4 protein cleanup comparison. To avoid experimental artefacts from buffer type and peripheral method differences, SP4 and centrifugal filters were adapted to follow the S-Trap procedure wherever possible. HEK293 lysate was prepared with 5% SDS, 50 mM triethylammonium bicarbonate (TEAB), sonicated as above, reduced with 5 mM TCEP for 15 min at 55 °C, and alkylated

with 20 mM CAA for 10 min. For S-Trap, the manufacturer's recommended protocol was followed: 100 μg was acidified, precipitated, and processed using S-Trap mini columns. For spin filtration, 20 μL (100 μg) of lysate in was applied to a pre-wetted nylon 0.22 μm spin filter and precipitated with 80 μL of ACN, precipitated captured and washed 3× with 80% ethanol at 6,000*g* for 1 min for all spins. For SP4-GB 80 μL of 12.5 μg/μL ACN–bead suspension was added to 20 μL (100 μg) of lysate and the described SP4 protocol followed. Digests were performed with 5 μg of trypsin and 2 μg of Lys-C in 125 μL of 50 mM TEAB for 2 h. Recommended S-Trap washes (80 μL of 50 mM TEAB, 0.2% FA, and 50% ACN) were used during all three methods, for the purposes of consistency. Though notably, this may have led to avoidable losses for SP4 from additional volumes and need for lyophilisation steps. Peptide solutions were lyophilised and reconstituted in 100 μL of 100 mM TEAB.

TMT labelling. For the 100 μg TMT experiments, 50 μL of 100 mM TEAB was used in place of ABC and both trypsin and Lys-C were added to a 1:100 enzyme:protein ratio. The resulting peptides were isolated by magnet or centrifugation and reaction vessels washed with 50 μL of 100 mM TEAB. 0.2 mg of TMT labeling reagent was added to each sample and incubated for 1 h at RT, and treated with 8 μL of 5% hydroxylamine for 15 min at RT. Labeled peptides were vacuum-concentrated, reconstituted, and pooled.

Peptide pre-fractionation. TMT-labeled peptides were reconstituted in 80 μL 3% (v/v) ACN + 0.1% (v/v) ammonium hydroxide and resolved using high-pH RP C18 chromatography (XBridge BEH 150 mm × 3 mm ID x 3.5 µm particle, Waters™, Milford, MA) at 0.3 mL/min with a Dionex UltiMate 3000 HPLC system (Thermo Scientific) at 30 °C. Mobile phases A (2% ACN + 0.1% ammonium hydroxide) and B (98% ACN + 0.1% ammonium hydroxide) were used for a gradient of: 0–20 min (3% B), 75 min (30% B), 105 min (85% B). 70 fractions were collected in a peak-dependent manner and individually lyophilized. Fractions at the extremes of the chromatogram were subjected to solid-phase extraction (SPE) and orthogonally concatenated, giving 62 fractions (TMT i) or 28 fractions (TMT ii–iv) for analysis.

LC-MS analysis. Label-free analyses of SP3, SP4-BF, and SP4-GB peptides were acquired using a Q-Exactive Plus Orbitrap MS (Thermo Scientific) coupled with a Dionex UltiMate 3000 nanoHPLC system (Thermo Scientific). Peptides were separated on a reversed-phase nanoLC column (150 mm × 0.075 mm; Reprosil-Pur C18AQ, Dr Maisch). For each analysis the equivalent of 100 ng peptides (as a proportion of protein input) were separated using a 120 min gradient of 5–35% ACN, 0.1% FA with a flow rate of ~300 nL/min.

Mass spectra were acquired with the following parameters for MS^1: resolution 70,000, scan range 350–1,800 m/z, automatic gain control (AGC) target 3×10^6, and maximum injection time 50 ms. MS^2 spectra for 2+ to 4+ charged species were acquired using: HCD fragmentation, top 10, resolution 17,500, AGC 5×10^4, maximum injection time 100 ms, isolation window 1.2 m/z, and normalized collision energy (NCE) of 27. The minimum AGC target was set at 2×10^3, which corresponds to a 2×10^4 intensity threshold.

TMT-labeled high-pH peptide fractions were analysed by Orbitrap Eclipse MS (Thermo Scientific) with on-line separation on a reversed-phase nanoLC column (450 mm × 0.075 mm ID) packed with ReprosilPur C18AQ (Dr Maisch, 3 μm particles) at 40 °C. A 60 min (TMT i) or 120 min (TMT ii–iv) gradient of 3–40% ACN, 0.1% FA at 300 nL/min was delivered via a Dionex UltiMate 3000 nanoHPLC system. Mass spectra were acquired in SPS MS^3 mode using a 3 s cycle time with the following settings: MS^1 — 120k resolution, max IT 50 ms, AGC target 400,000; MS^2 — IW 0.7 CID fragmentation, CE 35%, max IT 35 ms, turbo scan rate, AGC target 10,000; MS^3 — HCD fragmentation, CE 55%, 30k resolution, max IT 54 ms, AGC target 250,000.

Data analysis. LC-MS raw files were processed with Proteome Discoverer 2.5 using Sequest HT and Percolator, searching against UniProt Human Swissprot (UniProtKB 2021_01, canonical) and a PD

contaminant list (2015_5). Default settings were used, allowing 2 missed tryptic cleavages, with carbamidomethyl (C, fixed), oxidation (M, variable), acetyl/M-loss/M-loss+acetyl (protein N-term, variable), and, for the isobaric-labeled experiment, TMT 6-plex (K, peptide N-term, fixed). For 'complex' samples, the mouse (Swissprot, canonical) and *Drosophila melanogaster* (Swissprot and Trembl, canonical, 7227) proteomes were searched. For FFPE samples, methyl lysine was included as a variable modification. FTMS and ITMS spectra were searched with 0.02 and 0.5 Da fragment mass tolerances, respectively. Proteome Discoverer was used to determine protein and peptide identifications ($q < 0.01$), CV values, TMT quantitation and protein abundances. TMT ratios were determined without normalization (to assess technical effects), but corrected for batch-specific isotope impurities, with no imputation, minimum or missing values used. Minora feature detector was used for label-free quantitation. No normalization was applied to assess fully technical effects. Default setting were otherwise used. Proteome Discoverer was also used to assess differential protein recovery with *p*-values determined by multiple test-corrected *t*-test to determine the significance of observations of individual proteins across the replicates. One-way ANOVA and Tukey multiple comparisons test correction (GraphPad Prism 9.0) were used to determine significance between protein and peptide identification numbers (summarized in **Figure 1** and **Table S1**) with two-tailed Welch's *t*-test applied to paired analyses. R^2 values were determined as the squared Pearson product-moment correlation coefficient using Microsoft Excel. For the analysis of physicochemical property distributions, one-way ANOVA followed by Dunnett's multiple comparisons test, compared to the background TMT proteome, was performed to assess significant deviation from an expected distribution. Relative median protein recovery % was determined from the Proteome Discoverer and TMT-derived abundances calculated for each protein and isobaric label, with each percentage calculated relative to the highest reporter channel median protein abundance per 6-plex.

The MS proteomics data have been deposited to the ProteomeXchange Consortium (http://proteomecentral.proteomexchange.org) via the PRIDE partner repository (2) with the dataset identifier PXD032095 and, for validation work, PXD028736 and PXD028768. Proteomics data are summarised in **Table S1** and detailed in **Table S2-S20**.

Gene Ontology (GO) term enrichment analysis and functional annotation enrichment was performed with DAVID version 6.8. An addition analysis was performed with GO-SLIM. Terms were filtered to include those with Benjamini-adjusted significance ($p < 0.05$). Transmembrane proteins were defined by UniProt using the SUBCELLULAR LOCATION terms 'Single-pass type I membrane protein', 'Single-pass type II membrane protein', and 'Multi-pass membrane protein'. For protein solubility analysis, the UniProt Human Swissprot proteome was submitted to the CamSol Intrinsic tool for the calculation (at pH 7.0) of protein solubility and generic aggregation propensity, with a score generated for each protein sequence (3). Hydrophobicity (GRAVY score) was calculated by the PROMPT tool (4), and isoelectric points from ProteomePI (5).

Supplementary Methods for SP4 validation work (Figure 3 A–D)

Table S21. Summary of the methodologies used by each validation lab

	Lab 1		Lab 2	Lab 3
SP3 user	Yes		No	Yes
Protein input (*μ*g)	1, 10, 250	250	25	50
Sample type	Jurkat lysate	HEK293	HEK293	E14 murine ESC
Final protein conc. (*μ*g/*μ*L)	0.1, 0.5, 1.25	1	2.5	0.5
Replicates	*n* = 2/3	*n* = 3	*n* = 3	*n* = 5
Lysis buffer	RIPA		'SP3'	RIPA
Digestion method	Trypsin, O/N	Detailed above	Trypsin, O/N	Trypsin/Lys-C, 2 h, 70 °C
Other details	Acetone: overnight at −20 °C		-	Rapid digestion buffer
Peptide injection (ng)	100, 1000, 1000	1000	100	1000
MS	Fusion Lumos		QE+	QE HF-X
Data processing	Pulsar (Biognosys)		PD 2.1	MaxQuant

LAB 1

Lysate preparation (Experiment 1)

Jurkat immortalized human T cell lysate was prepared and diluted with RIPA lysis buffer (150 mM NaCl, 1.0% IGEPAL CA-630, 0.5% sodium deoxycholate, 0.1% SDS, 50 mM HEPES, pH 8.0, Protease inhibitor cocktail, (Calbiochem set III, 539134)) to 1.25 *μ*g/*μ*L. Three different masses of Jurkat protein lysate in RIPA lysis buffer were prepared: 250 *μ*g (1.25 *μ*g/*μ*L) ,10 *μ*g (0.5 *μ*g/*μ*L), and 1 *μ*g (0.1 *μ*g/*μ*L). Each experiment was performed as discrete technical triplicates, e.g., with 3 separate aliquots of 250 *μ*g of protein processed for each method.

† In the case of Fig 3A (1 *μ*g, acetone overnight, and SP4-GB), only two experiments are present due to a technical failure during the injections of the entire 1 *μ*g peptide sample, resulting in no material remaining for a repeat injection.

Sample preparation (Experiment 1)

Treatment. Cell lysate was reduced with 5 mM DTT (30 min at 25 °C) and then treated with 5 mM iodoacetamide (30 min, 25 °C in the dark). Proteins were recovered by one of the four methods:

Acetone Precipitation. Proteins were precipitated by adding ice-cold acetone (4× sample volume, overnight, −20 °C). Protein pellets were obtained by centrifugation (18,000*g* for 10 min at 4 °C) and washed (2×) with the same volume of ice-cold 80% acetone/water (with sonication between washes). The final wash liquid was aspirated, and samples were air-dried for 20 min. Each sample was resuspended in 50 mM HEPES (250 *μ*L for 250 *μ*g and 20 *μ*L for 10/1 *μ*g). Samples were sonicated and vortexed to re-dissolve the pellet.

Seramag SP3 Beads. A stock of SP3 beads was prepared at 50 mg/mL by combining equivalent volumes of hydrophobic bead slurry and hydrophilic bead slurry. The resulting slurry was washed (3×) water, (3×) 50 mM HEPES. SP3 beads were added to cell lysate in bead:protein ratio of 10:1 (w/w) and distributed through gentle pipetting. The volume of the mixture was doubled with absolute ethanol and shaken (800 rpm for 10 min at RT). Tubes were placed on the magnetic separator and allowed to separate. The protein–bead aggregates were washed 3× while remaining on the magnetic rack with an equivalent total precipitating reaction volume of 70% ethanol/water (for 1 *μ*g: 20 *μ*L, 10 *μ*g: 40 *μ*L, and 250 *μ*g: 400 *μ*L) and then gently reconstituted by pipette with 50 mM HEPES to a final concentration of 250 *μ*g (1.0 *μ*g/*μ*L), 10 *μ*g (0.5 *μ*g/*μ*L), and 1 *μ*g (0.1 *μ*g/*μ*L).

ReSyn HILIC Beads. A stock of MagReSyn HILIC beads (ReSyn Biosciences) was supplied at 50 mg/mL. The resulting slurry was washed with water (3×) and 50 mM HEPES (3×). ReSyn beads were added to cell lysate in bead:protein ratio of 10:1 (w/w) and distributed through gentle pipetting. The volume of the mixture was doubled with 200 mM ammonium formate pH 4.5, 30% ACN mixtures (binding buffer), and the tubes were shaken (800 rpm for 30 min). Tubes were placed on the magnetic separator and allowed to separate. The protein–bead aggregates were washed 3× while remaining on the magnetic rack with an equivalent total precipitating reaction volume of 95% ACN (for 1 μg: 20μL, 10 μg: 40 μL and 250 μg: 400 μL) and then gently reconstituted by pipette with 50 mM HEPES to a final concentration of 250 μg (1.0 μg/μL), 10 μg (0.5 μg/μL), and 1 μg (0.1 μg/μL).

Glass Beads. 100 mg of glass beads was distributed in 1 mL of Ultrapure water. This slurry was vortexed and centrifuged (16,000*g* for 2 min at 4 °C). The buoyant beads were gently aspirated to leave a glass bead pellet. This process was repeated with ACN (1×), 50 mM HEPES (1×) and Ultrapure water (2×). On the final wash, beads were resuspended in 1 mL of Ultrapure water, and a bead concentration of 50 mg/mL was assumed. Glass beads were added to cell lysate in bead/protein ratio of 10:1 (w/w) and distributed through gentle vortexing. ACN was added to a final concentration of 80%. Upon addition of ACN, the mixture was again gently vortexed and then the tubes were centrifuged (16000*g* for 3 min at 4 °C (2×, with tubes spun in between)). The liquid was gently aspirated, and the beads were washed 3× with the equivalent volume of 80% ethanol/water (for 1 μg: 50 μL, 10 μg: 100 μL, and 250 μg: 1000 μL). Beads were reconstituted with additional sonication with 50 mM HEPES to a final concentration of 250 μg (1.0 μg/μL), 10 μg (0.5 μg/μL), and 1 μg (0.1 μg/μL).

Digestion. For the solely trypsin samples, digestion with trypsin (1:100 enzyme/protein; Promega) was carried out overnight at 37 °C.

Recovery of Peptides from Beads

Seramag SP3 Beads / ReSyn Beads. Tubes were placed on the magnetic separator and the peptide mixture was carefully pipetted off and dispensed into a fresh microcentrifuge tube.

Glass Beads. Tubes were centrifuged (16,000*g* for 3 min at 4 °C (2×, with tubes spun in between)) and the peptide mixture was carefully pipetted off and dispensed into a fresh microcentrifuge tube.

Lysate Preparation (Experiment 2)

HEK293T lysate was prepared and diluted with RIPA lysis buffer to 1.25 μg/μL. 250 μg samples were prepared at 1 μg/μL and each experiment was performed at least in biological triplicate.

Sample Preparation (Experiment 2)

Treatment. Cell lysate was reduced with 5 mM DTT (30 min at 25 °C) and then treated with 5 mM iodoacetamide (30 min at 25 °C in the dark). Proteins were then recovered by one of the two methods:

Acetone Precipitation. An analogous procedure to Experiment 1 was used up to point of re-dissolving the pellet. Each pellet was resuspended in the following volumes and buffers: 250 μL of 50 mM HEPES for trypsin only and 125 μL of 50 mM HEPES with 1 M guanidinium hydrochloride for Lys-C/trypsin. Samples were sonicated and vortexed periodically to re-dissolve the pellet.

Glass Beads. An analogous procedure to Experiment 1 was used up to point of reconstituting the beads. Beads were re-distributed *via* sonication with the following volumes and buffers: 250 μL of 50 mM HEPES for trypsin only and 125 μL of 50 mM HEPES with 1 M guanidinium hydrochloride for Lys-C/trypsin. Tubes were centrifuged (16,000*g* for 3 min at 4 °C (2×, with tubes spun in between)) and the peptide mixture was carefully pipetted off and dispensed into a fresh microcentrifuge tube.

Digestion. For the solely trypsin samples, digestion with trypsin (1:100 enzyme/protein; Promega) was carried out overnight at 37 °C.

For the Lys-C/trypsin samples, digestion with Lys-C (1:100 enzyme:protein; Wako) was carried out for 4 h at 37 °C, followed by 1:2 dilution with 50 mM HEPES and a secondary digestion with trypsin (1:100 enzyme:protein; Promega) performed overnight at 37 °C.

Data Acquisition (Both Experiments)

Assuming 100% recovery, 1 μg of each peptide mixture was added to 200 μL of 0.1% formic acid on a prepared Evotip (Evosep Biosystems) and run on an Evosep One LC connected to the Orbitrap Fusion MS instrument using 44 min LC-MS/MS gradient in DDA mode as described: the transfer capillary set to 300 °C and 2.2 kV applied to the nanospray needle (Evosep Biosystems). MS^1 data was acquired in the Orbitrap Fusion with a resolution of 60k, a max injection time of 20 ms, and an AGC target of 1×10^6, in positive ion mode, with profile spectra, over the mass range 375–1200 m/z. A charge state inclusion of precursors with 2–6+ charges was applied with the MIPS mode (Peptide) active, a dynamic exclusion of 15 s, intensity threshold of 5×10^4, and isolation carried out in the quadrupole with a width of 1.4 Da. For fragmentation, HCD energy of 32% was applied and MS^2 were acquired in the Orbitrap with 15k resolution, max injection time of 22 ms and an AGC target of 1×10^6 in centroid mode.

Data Analysis (Both Experiments)

For sample-specific spectral library generation, data was acquired from samples from each condition in data-dependent acquisition (DDA) mode. The data were searched against the human Uniprot database using the Pulsar search engine (Biognosys AG). The following modifications were included in the search: Carbamidomethyl (C) (Fixed) and Oxidation (M)/Acetyl (Protein N-term) (Variable). A maximum of 2 missed cleavages for trypsin were allowed. The identifications were filtered to satisfy FDR of 1% on peptide and protein level. Protein Group, Peptide and Precursor numbers were reported based on the library generated by the search.

LAB 2

Same as in main methods, with 3× 25 μg (10 μL of 2.5 μg/μL) preparations of HEK293 lysate for SP3, SP4-BF and SP4-GB.

LAB 3

Comparison of SP3 and SP4 sample processing methods. E14 murine embryonic stem cells were lysed in RIPA buffer (150 mM NaCl, 1.0% IGEPAL CA-630, 0.5% sodium deoxycholate, 0.1% SDS, 50 mM Tris, pH 8.0) by pipetting and sonication. The lysates were clarified by centrifugation (20,000*g* for 10 min at 4°C) and protein concentrations were determined by BCA assay. Aliquots (n = 5 per experimental condition) corresponding to 50 μg of total protein were removed and diluted (1:1) with 20 mM HEPES, pH 8.5 buffer. Reduction with 5 mM TCEP final concentration was carried out at 37 °C for 45 min and alkylation with 20 mM 2-chloroacetamide (30 min at 25 °C). SP3 and SP4 protocols were carried out as described in the main methods. Following the respective processing methods, rapid digestion buffer (150 μL per sample, Promega VA 1061) was added followed by 5 μg Lys-C/trypsin mixture (Promega VA1061). Protein digestion was carried out at 70 °C with shaking (800 rpm) for 2 h. Samples were removed from the incubator and cooled on ice. Acidification was achieved by addition of

10% TFA (final concentration: 0.25%) and glass or magnetic beads were removed by centrifugation (20,000*g* for 5 min at 25 °C). Supernatants were transferred to sample vials and analysed by LC-MS/MS.

Liquid chromatography-tandem mass spectrometry (LC-MS/MS) analysis. Sample aliquots corresponding to 1 μg total digest were injected on a U3000 RSLC nano-liquid chromatography system onto a trapping column (Thermo Acclaim Pepmap 100, 0.1 mm × 20 mm, 164564) at a flow rate of 8 μL/min with loading buffer (2% ACN, 0.1% TFA). Following valve switch peptides were eluted onto an analytical column (Thermo EasySpray column, 0.075 mm × 500 mm, ES803A) by applying a linear multi-step gradient (buffer A: 5% DMSO, 0.1% formic acid; buffer B: 75% ACN, 5% DMSO, 0.1% formic acid) at a flow rate of 250 nL/min and a column temperature of 40 °C: 1% B [0–5 min], 22% B [75 min], 42% B [95 min], 87% B [95.1 min]. The elution gradient was followed by column wash and equilibration steps.

The Q-Exactive HF-X mass spectrometer was operated in positive ionisation mode at a spray voltage of 1.6 kV. DDA was carried out with a top 30 method, automatic gain control targets of 3×10^6 (MS^1) and 5×10^4 (MS^2) ions and maximum accumulation times of 25 ms (MS^1) and 50 ms (MS^2), respectively. Dynamic exclusion of fragmented precursors was enabled for 50 s.

Data processing and analysis. Raw data files were processed with MaxQuant version 1.6.10.43 and database searches carried out against a Swissprot *Mus musculus* database (version 2020.11.11, 17,056 entries). Settings included trypsin digestion with up to two missed cleavages, and a false discovery rate (FDR) of 1% for peptide spectrum matches and protein identifications. Protein N-terminal acetylation, methionine oxidation and peptide N-terminal glutamine to pyroglutamate conversion were enabled as variable modifications and cysteine carbamidomethylation as a fixed modification. The 'match between runs' option was enabled within experimental conditions (SP3 or SP4 digests) with match and alignment time windows of 0.7 and 20 min, respectively.

Supplementary References

1. Doellinger J, Schneider A, Hoeller M, Lasch P. Sample Preparation by Easy Extraction and Digestion (SPEED) - A Universal, Rapid, and Detergent-free Protocol for Proteomics Based on Acid Extraction. Mol Cell Proteomics. 2020;19(1):209-22.
2. Perez-Riverol Y, Csordas A, Bai J, Bernal-Llinares M, Hewapathirana S, Kundu DJ, et al. The PRIDE database and related tools and resources in 2019: improving support for quantification data. Nucleic Acids Res. 2019;47(D1):D442-D50.
3. Sormanni P, Aprile FA, Vendruscolo M. The CamSol method of rational design of protein mutants with enhanced solubility. J Mol Biol. 2015;427(2):478-90.
4. Schmidt T, Frishman D. PROMPT: a protein mapping and comparison tool. BMC Bioinformatics. 2006;7:331.
5. Kozlowski LP. Proteome-pI: proteome isoelectric point database. Nucleic Acids Res. 2017;45(D1):D1112-D6.

SP4 (Solvent precipitation SP3) protocol

Glass bead preparation (optional):

- 9–13 *μ*m glass spheres/beads
  (e.g., https://www.sigmaaldrich.com/catalog/product/aldrich/440345)
  Glass beads broadly improved recovery, digestion efficiency and reproducibility, but are not required
- Suspend 100 mg in 1 mL of Ultrapure water, vortex until suspended fully, and pellet at > 500*g* for 1 min.
  Of note: approximately 50% of the beads are buoyant, and will not pellet, and should be removed over the course of these wash steps. Additionally, small amounts of metal in the beads can be removed by magnet or acid wash but had no effect on the performance of the beads. Larger scale preps are possible but may require additional washes due to buoyant beads.
- Resuspend, vortex and wash with ≥ 1 mL of: 100% acetonitrile (ACN) (1×), 100 mM ABC* (1×), and Ultrapure water (≥ 2×) ensuring no unpelleted beads remain. * or equivalent digestion buffer.

Then either:

- **A.** Resuspend beads in 0.9 mL of Ultrapure water to 50 mg/mL.
  given ~50% of beads are retained

or

- **B.** Resuspend beads in 0.9 mL acetonitrile to 50 mg/mL (recommended).
  - Avoids protein dilution from beads in water.
  - Ensures uniform bead dispersion
  - Dilute beads to at least 2.5× [protein] (so bead:protein is 10:1 from 4 volumes of bead–ACN suspension)

This will be sufficient to prepare 50 mg of protein—excess can be stored at 4 °C.
(with 0.2% sodium azide, if in water for an extended period)

Lysate/protein solution prep recommendations

- SP4 is broadly compatible with the majority of lysis buffers as for SP3 or acetone precipitation
  Tested with:
  - 5% total detergent ‘SP3 lysis buffer’
    - (50 mM HEPES pH 8, 1% SDS, 1% Triton X-100, 1% IGEPAL CA-630, 1% Tween 20, 1% sodium deoxycholate, 50 mM NaCl, 5 mM EDTA, 1% (v/v) glycerol, and 1× protease inhibitors)
  - 8 M urea (diluted to 2 M prior to ACN addition)
  - TFA/Tris diluted 1:1 with water as described for the ‘SPEED’ method
- For best results with SP4, protein concentration should be as high as possible (0.25–5 *μ*g/*μ*L).
  - For lower concentrations or where highest possible recovery is required, longer precipitation reactions, carboxylate-modified beads, pre-chilled ACN, and centrifugation at 4 °C may help yields.
- DNA shearing (e.g., by sonication), protease inhibitors, & lysate clearance are recommended.

SP4 protocol recommendations

- The use of the smallest possible tube will help create a denser pellet, e.g., 500 *μ*L tube for samples of less than 50 *μ*L.
- Liquids should be kept low in the tube, with losses/contamination possible from tube walls/lid.
- Set vortex to < 500 rpm for very gentle mixing.
- Pipette ACN directly into the sample to ensure rapid mixing, but do not touch the ACN–sample mix with the tip.
- Use the tube hinge to orientate the location of the pellet (fixed angle rotors).
  - Initially orientate the tube hinge inwards during the pellet precipitation and turn 180° after 2.5 min will give a denser pellet and less risk of loss from fragile wall adhesion.
- During wash removals, avoid touching the tube walls with the tip as precipitation may occur on them, pipette slowly and avoid agitating the pellet.
- If adding beads, ensure they maintain a uniform suspension in water/ACN by pipetting up and down at least once between additions.
- Organic solvent for aggregation/washes appears interchangeable between ethanol, ACN, IPA, & acetone (Ref. 2).

SP4 Protocol

1. Aliquot reduced/alkylated protein mixture/lysate into a fresh LoBind-type microcentrifuge tube.
    - Volumes and conditions are given for the example of 10 μg protein in 10 μL of 1 μg/μL lysate.
2. Options (choose one):

2a. Bead-free

- Add 4 volumes of ACN.
    - E.g., 40 μL for 10 μL sample

2b. Glass beads (in water)

- Add 50 μg/μL beads (water-suspended) at 10:1 beads:protein and vortex.
    - E.g., 100 μg (2 μL) beads
- Add 4 volumes of ACN
    - E.g., 48 μL to 12 μL sample:bead mix

2c. Glass beads (in ACN) (recommended)

- Adjust beads to 2.5× protein concentration.
    - E.g., 2.5 μg/μL for 1 μg/μL sample
- Add 4 volumes of this ACN:bead suspension.
    - E.g., 40 μL for 10 μL sample

3. Ensure complete mixing (without pipette mixing, e.g., by consistent ACN addition, or < 500 rpm vortex for 5 s).
4. Centrifuge for 5 min at 500–16,000*g*.
5. Remove supernatant by pipetting slowly and remove a consistent volume of 90–95%. Avoid disturbing beads/pellet.

    E.g., for a 50 μL total precipitation reaction remove 45 μL

6. Wash with 80% ethanol, volume ≥ 1.5× total precipitation volume (or at least 180 μL)
    - Pipette gently down the side opposite the hinge/pellet to avoid disturbance, do not vortex/resuspend.
7. Centrifuge for 2 min at 16,000*g*.
8. Remove 90–95% of wash.

    E.g., leaving ~5–10 μL during washes

9. Repeat wash steps for a total of 3 washes.
10. Remove >= 95% of final wash.
    - For larger volumes a final 2 min spin will help with removal of excess wash.

    E.g., leaving < 5 μL after final wash aspiration

11. Add preferred digestion buffer, e.g., 20–100 mM ABC or TEAB (pipette mixing will cause losses)
12. Add preferred digestion enzyme, e.g., trypsin/Lys-C at a 1:10 to 1:100 enzyme:protein ratio.
    - A digestion buffer/enzyme master mix will reduce variability and simplify pipetting—keep on ice.
    - Use a volume equivalent to ~0.5–2× the total precipitation volume.

        E.g., 25–100 μL for 50 μL precipitation reaction

    - In-bath sonication (5–10 min) can help to disrupt the pellet and increase surface area.
    - Larger bead-free pellets may require additional agitation to resuspend but keep sample low in tube.
    - 18 h digestion consistently worked without pellet resuspension for < 25 μg protein.
13. Incubate in a Thermomixer at 1000 rpm at desired conditions, e.g., for 18 h at 37 °C.
    - Beads were compatible with 2 h @ 47 °C using 1:10 trypsin or 2 h @ 70 °C (rapid digestion buffer), ensuring resuspension

Peptide collection

- Centrifuge the peptide mixture at 500–16,000*g* for 2 min & collect peptide supernatant.
- For maximum recovery, rinse pellet/tube in an equal volume of digestion buffer added above.
    - A final centrifugation step may be required to ensure no beads are carried over.
- Peptides solution at this stage is clean enough to be:
    - Acidified (e.g., by 0.1–1% formic acid or trifluoroacetic acid) for direct LC-MS injection.
    - Dried by vacuum concentration to provide near-pure peptides.

Protocol References

1. Hughes CS, Moggridge S, Muller T, Sorensen PH, Morin GB, Krijgsveld J. Single-pot, solid-phase-enhanced sample preparation for proteomics experiments. Nat Protoc. 2019;14(1):68-85.
2. Moggridge S, Sorensen PH, Morin GB, Hughes CS. Extending the Compatibility of the SP3 Paramagnetic Bead Processing Approach for Proteomics. J Proteome Res. 2018;17(4):1730-40.
3. Dagley LF, Infusini G, Larsen RH, Sandow JJ, Webb AI. Universal Solid-Phase Protein Preparation (USP(3)) for Bottom-up and Top-down Proteomics. J Proteome Res. 2019;18(7):2915-24.
4. Batth TS, Tollenaere MAX, Ruther P, Gonzalez-Franquesa A, Prabhakar BS, Bekker-Jensen S, et al. Protein Aggregation Capture on Microparticles Enables Multipurpose Proteomics Sample Preparation. Mol Cell Proteomics. 2019;18(5):1027-35.
5. Sielaff M, Kuharev J, Bohn T, Hahlbrock J, Bopp T, Tenzer S, et al. Evaluation of FASP, SP3, and iST Protocols for Proteomic Sample Preparation in the Low Microgram Range. J Proteome Res. 2017;16(11):4060-72.
6. Holger lab (MRC unit) SOP.